

Bachelor Thesis:

Electrodeposition of Gold (Au) for Transition Edge Sensor ATHENA +

Technische Natuurkunde (HHS)/ Applied Physics (The Hague University of Applied
Sciences)



SRON
Netherlands Institute for Space Research

DE HAAGSE
HOGESCHOOL

Kerim Vonk
Supervisor SRON: M. Ridder
Supervisor HHS: C.A. Swarts
10-4-2015

Summary

The aim for this thesis is to set up and develop electroplating technique for depositing gold layers. This gold layer will be used as an thermalisation layer in a cryogenically cooled X-ray detector. Key material parameter for the gold layer is a low thermal resistivity at cryogenic temperatures. Since electroplating seemed to be the appropriate deposition technique SRON started up electroplating experiments to deposit gold.

Within this thesis a literature study has been worked out on resistivity at low temperature and on the basic principles of electroplating technique. The experimental part of this thesis comprises the setup and the deposition of gold layers by electroplating. In addition the gold layers were tested and characterized on resistivity at room temperature and at cryogenic (4.2 kelvin) temperature.

The experimental part was an important aspect of this study, particularly establishing a stable setup for the electrodeposition of the gold layers. The plating bath characterization was obtained by conducting an Cyclic Voltammetry. The next characterization was done by determining the amount of bath agitation by mechanically stirring the electrolyte, it was found out that a stirring rate of 500 rpm was sufficient to obtain reproducible depositions. The last characterization was done by assessing the difference between electroplating using current bias or voltage bias. It turned out that current bias showed better reproducibility of the deposited gold layers and their thickness.

With the characterized plating bath defined the plating parameters could be optimized to deposit gold layer with the preferred resistivity values. First the resistivity values of the deposited layers were measured room temperature, then a selection was measured at temperature of 4 Kelvin.

The resistivity at room temperature was found to be around $3 \mu\Omega\text{-cm}$ which was slightly higher than values demonstrated by other groups. At low temperature we measured resistivity values from $0.3 \mu\Omega\text{-cm}$ till $0.46 \mu\Omega\text{-cm}$. The lowest value was achieved by using electrolyte without the additive 'brightener'. We assumed that this can be related to larger grain sizes in the microstructure of the gold layer. Compared to other groups the lowest resistivity value we have measured is still a factor of 6 higher than demonstrated by other groups.

Therefore more tests have be done with the electrolyte without brightener. This thesis will also give some suggestions how to proceed a further optimization process.

Table of contents

Summary.....	1
Table of contents.....	2
1 Introduction	3
2 Fundamentals of resistivity and electrodeposition	4
2.1 Introduction	4
2.2 Thermal conductivity	5
2.3 Electrical resistivity.....	5
2.4 Electrochemistry of Gold plating	10
3 Experimental setup.....	16
3.1 Electroplating setup	16
3.2 Diagnostic tools.....	18
4 Experimental results.....	20
4.1 Bath characterization	20
4.2 Comparison of various plating conditions.....	22
4.2 Effect of layer thickness on the resistivity	25
4.5 Effect of Brightener	27
5 Discussion.....	29
6 Conclusion.....	32
Literature	33
Appendix	34
A. Originele opdracht omschrijving	34
B. Mathematical derivation of Electrical resistivity.....	35
C. Data sheet NB Semiplate AU 100.....	36
D. Technical data Autolab PGSTAT204	41
E. Measured data of deposited test structures	0

1 Introduction

The European Space Agency's (ESA) Advanced Telescope for High- Energy Astrophysics or ATHENA is set to launch in 2028. This telescope will be designed to address the cosmic science theme 'The hot and energetic universe' and poses two key astrophysical questions^[1]:

- How does ordinary matter assemble into the large-scale structures we see today?
- How do black holes grow and shape the universe?

The ATHENA spacecraft will be composed of three key elements:

- An X-ray telescope with a focal length of 12 m and an effective area of $\sim 2 \text{ m}^2$ at 1 keV
- An X-ray Integral Field unit (X-IFU) for high-spectral resolution imaging
- A Wide Field Imager (WFI) for high count rate, moderate resolution spectroscopy over a large field of view.

The X-IFU detector will be composed of a large array of Transition Edge Sensors (TES). TES sensors can absorb X-ray Photons and convert these to thermal energy which will result in a minute rise in temperature and this is measured by the sharp change in the electrical resistance of the TES. To achieve the required edge in resistance the TES will be composed of a Titanium/Gold (Ti/Au) layer cooled to a temperature of 100 mK and biased into its transition between superconducting and normal state.

SRON (Netherlands Institute for Space Research) stated its research on the TES sensors in 1996 and is currently developing the TES sensors for ESA's ATHENA+ mission. The challenging requirements on the sensitivity of the X-IFU detector still require further optimization of the TES detectors. One of the properties of the TES sensors to be further optimized is the thermal conduction of the Au thermalisation layer as shown in figure 1.

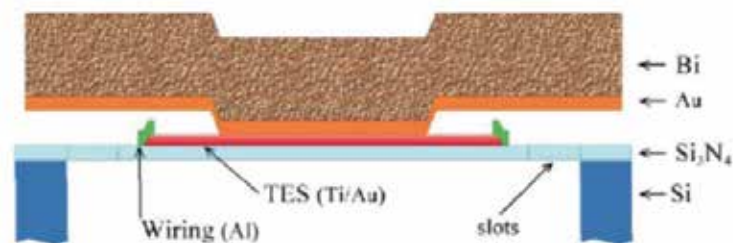


Figure 1: Cross section of the Transition Edge Sensor (TES). The TES will be composed of a Titanium/Gold layer biased into its transition between superconducting and normal state. The Absorption layer will be composed of a Bismuth/Gold layer. The Bi layer will be designed to be the main absorber and the gold layer functions as a thermalisation layer between the absorber and the TES.

The TES will be composed of a thin superconducting metal and a thicker layer designed to absorb approximately 95% of the incident x-ray photons. This absorption layer should have a low heat capacity and high X-ray stopping power. Around $6 \mu\text{m}$ of Bismuth is a good choice, but has a too low heat conduction. therefore the Bi should be combined with a thinner gold layer of around $1 \mu\text{m}$ thick. The high heat conductive gold layer will transport the absorbed energy of the incident photons to the Ti/Au thermometer. For the detector to function respond in an uniform way a fast internal thermalisation at cryogenic temperature of the gold layer is required. SRON has various in-house facilities to deposit Au layers, like E-beam evaporation and sputter coating, but various groups showed that gold deposited using electroplating have the highest heat conductivity at cryogenic temperature.^[2,3]

The aim of this thesis work is to optimize the electroplating process and to produce gold layers with the desired thermal conductivity at cryogen temperatures. The electroplated gold layers will be analyzed at room temperature and at cryogen temperatures. The thermal and electrical properties are strongly related through the Wiedemann-Franz law, and therefore the Au layers will be characterized on their electrical resistivity at both room and cryogen temperature.

2 Fundamentals of resistivity and electrodeposition

2.1 Introduction

The following chapter will give an insight in the physical mechanisms involved in the conduction of thermal energy and electric conduction through a material and the basics of the electro-chemical process of electroplating.

Conducting materials possess "free electrons" or conduction electrons and these can move freely through the material and are the main source of thermal conductivity as well as electrical conductivity. The relation between these two conductivities is described by the Wiedemann-Franz law. The electrical conductivity is an easily measured physical property compared to thermal conductivity measurements. Therefore the thermal conductivity will be assessed by measuring the electrical resistance of the deposited Au layer. The electrical resistance will then be used to calculate the electrical resistivity of the deposited Au layer.

To get a better insight on the electrical, and the related thermal, conductivity the origin of a materials resistivity to the movement of "free electrons" will be discussed. The various influencing factors like temperature, the purity and the microstructure of the deposited Au layer on the electrical resistivity will be discussed. When the mean free path of the conducting electrons becomes comparable to the layer thickness scattering of conduction electrons at the conducting materials surface will become a dominant factor in the total resistivity. To better understand this effect the solid state physics of thin film will have to be analyzed. The Residual Resistivity Ratio (RRR) is the ratio between the room temperature and cryogenic temperature resistivity and can be seen as an indication for the purity of a material.

Electroplating has been around for over a century, has been studied extensively and a wide variety of electrolytes are commercially available. To better understand the electro-chemical processes involved in electroplating the basics of electrodeposition will be discussed. The methods used for the characterization of the electrolyte used for the deposition of the Au layer will be discussed as well. The grain size of the deposited gold layers is a key factor for the thermal and electrical resistivity at both room and cryogen temperatures. This grain size is controllable through a number of electroplating parameters. The main parameters under discussion are the applied current density, bath agitation and bath temperature. By varying these parameters the optimal plating conditions for electroplating gold layers with good thermal and electrical resistivity can be obtained.

2.2 Thermal conductivity

The thermal conductivity of materials can be categorized in multiple mechanisms. The transfer of heat through gasses is low compared to heat transfer in most solids and is caused by direct collisions between molecules. The heat transfer in non-metallic solids is caused by lattice vibrations or "phonons". Metals are far better thermal conductors than non-metals and this is caused by the fact that the "free electrons" which participate in the electrical conductivity also take part in the transfer of heat. The electrical resistivity is easily measured at room and cryogenic temperatures using an electrical circuit and therefore the thermal resistivity is analyzed by measuring the electrical resistivity. The relation between the electrical and thermal conductivity is called the Wiedemann-Franz law and follows^[2]:

$$\frac{k}{\sigma} = LT \quad [1]$$

where:

k	= Thermal conductivity	[W/mK]
σ	= Electrical conductivity	[1/Ωm]
L	= Lorenz number	[$2.44 \cdot 10^{-8}$ WΩ/K]
T	= Temperature	[K]

2.3 Electrical resistivity

The electrical resistivity of a material is an intrinsic property. The resistivity is a rate at which a material works against an electrical current. Materials with a low resistivity have little resistance for an electrical current. The resistivity of a given material can also be expressed in the conductivity. The conductivity is the reciprocal of the resistivity and stands for the rate at which a given material conducts an electrical current. If a current is applied onto a conducting bar with known resistance the voltage drop over this bar can be calculated. This relation is called Ohm's law and is as followed:

$$\Delta V = I \cdot R \quad [2]$$

where:

ΔV	= Voltage difference	[V]
I	= Electrical current	[A]
R	= Electrical resistance	[Ω]

The resistance depends on the geometry of the bar and the properties of the conducting material. To define the material property that fixes the electrical resistance the relation between these will have to be found. Let's consider a thin wire and define the current density as the following:

$$J = \frac{I}{A} \quad [3]$$

where:

J	= Current density	[A/m ²]
A	= Cross-section area	[m ²]

The voltage difference across this thin wire can then be defines as followed:

$$E = \frac{\Delta V}{L} \quad [4]$$

where:

$$\begin{aligned} E &= \text{Electric field strength} && [\text{V/m}] \\ L &= \text{Length of the wire} && [\text{m}] \end{aligned}$$

By rearranging formula 2,3 and 4 Ohms law can be written as the following:

$$E = \frac{R \cdot A}{L} \cdot J \quad [5]$$

The electrical resistivity is then defined by the following relation:

$$\rho = \frac{R \cdot A}{L} \quad [6]$$

where:

$$\rho = \text{Electrical resistivity} \quad [\Omega \cdot \text{m}]$$

To get a better insight in the origin of the intrinsic material property that is the electrical resistivity one has to take a closer look at the mechanisms involved in electrical conduction. In the vast majority of materials the conduction of electricity is due to the flow of electrons. The other mechanisms like diffusion of ions in ionic materials and conduction trough "holes" in semiconductors will not be discussed in this paper.

The origin of a material's electrical resistivity can be found by considering conducting electrons as particles. A conductive material possesses "free" electrons and these can be accelerated under influence of an electric field. These drifting electrons can collide with the lattice atoms (electrostatically interact) and therefore lose some of their energy. The drifting electrons are said to move through the material in a zigzag path as sketched in figure 2. The average distance the conducting electrons travel thought he material is thus related to the resistivity of the material and is called the mean free path. When the temperature of the material rises the lattice atoms increasingly oscillate around their equilibrium positions due to the supply of thermal energy. This increase in oscillation increases the chance the electrons collide and in turn increases the loss of energy. The resistivity of a material will however not vanish at near zero temperatures. This is due to the different imperfections and impurities in a crystal structure and is temperature independent.^[5] Further mathematical derivation of the origin of the resistivity can be found in appendix B.

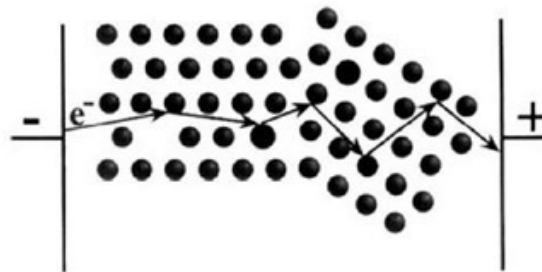


Figure 2: Schematic representation of the path of an conducting electron trough a conductive material. The conducting electron moves in a zigzag trough the material due to imperfections and vibrations of the lattice atoms.^[5]

2.2.1 Influence of temperature and purity

As stated in the previous paragraph the resistivity of a material originates from the interactions of the conducting electrons with lattice vibrations and impurities in the crystal structure of the material and is related to the mean free path. These are two separate mechanisms that contribute to the total resistivity of a material. These individual resistivity's add to form the total resistivity through Matthiesen's rule:^[11]

$$\rho = \rho_{lat} + \rho_{imp} \quad [7]$$

where:

$$\begin{aligned} \rho_{lat} &= \text{Resistivity induced by lattice atom vibrations} && [\Omega \cdot \text{m}] \\ \rho_{imp} &= \text{Resistivity induced by imperfections and defects} && [\Omega \cdot \text{m}] \end{aligned}$$

let's consider a material with a material with a crystal structure which contains no defects or impurities. The only source of scattering of the conducting electrons in this material will be off of lattice atom vibrations due to the thermal energy of these atoms. The relation between the thermally induced resistivity is linear with the temperature of the conducting material. The thermally induced resistivity can be calculated using the following equation:

$$\rho_{lat} = \rho_1(1 + \alpha(T_2 - T_1)) \quad [8]$$

where:

$$\begin{aligned} \alpha &= \text{Temperature coefficient of resistivity of gold} && [34 \cdot 10^{-4} \Omega \text{m/K}] \\ T &= \text{Absolute temperature} && [\text{K}] \end{aligned}$$

In practice however, the crystal structure of a metal always contains mechanical imperfections such as dislocations, grain boundaries, small clusters and impurities in the material. The contribution of these imperfections on the resistivity are temperature independent and the remaining resistivity at cryogen temperature will be determined by ρ_{imp} , as shown in figure 3. The resistivity at room temperature will be dominated by ρ_{lat} .

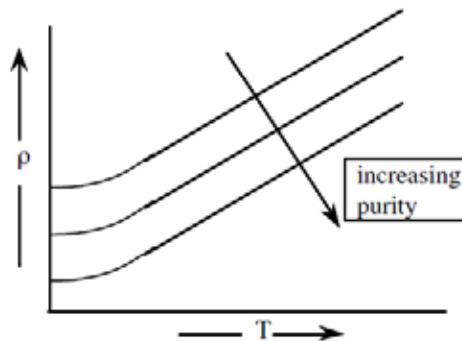


Figure 3: Total resistivity. A higher purity and less imperfections shifts the entire resistivity downwards.^[6]

Since ρ_{imp} depends on the purity of the metal film and ρ_{lat} is temperature independent, the ratio of the resistivity at room temperature and at 4 Kelvin often serves as a good practical measure of the purity and perfection of the metal. In a very pure metal that is free of distortion, this *resistivity ratio* can be as high as 10^4 to 10^5 . In impure metals, it may be below 10. In the next paragraph the effect of grain boundaries will be discussed. since grain boundaries are one of the known contribution of imperfections,

2.2.1.2 Grain boundaries

Grain boundaries occur where the crystallographic direction of the lattice abruptly changes direction. This usually occurs when two crystals begin growing separately and then meet, resulting in perfect crystal structures stacked onto each other with random orientation. The border between these differently oriented crystal structures are large areas of interruptions of the systematic structure of the crystal structure. These borders provide large areas at which the conducting electrons are able to scatter and thus lose some of their energy. When the size of the individual grains grows, the number of boundaries and thus the number of scattering areas will decrease. Scattering of conducting electrons off of grain boundaries becomes an influencing factor on the total resistivity if the mean free path of the conducting electrons is in the order of magnitude of the size of these grains. When we consider the mean free path of the electrons becomes large enough, the mean free path becomes limited by the size of these grains.

The relation between the concentration of grains in copper wires and the resistivity at room temperature has been studied by Yan Wen, CHEN Jian and FAN Xin-hui.^[7] This paper shows a non-linear relation between the concentration of grains and the total resistivity for copper wires. The effect of grain boundaries becomes more evident as the temperature of the material drops. At cryogenic temperatures the thermal vibration of the lattice atoms disappears and the electron mean free path will be limited by the impurities and defects in the material only. In this temperature region the grain size will have a profound effect on the electron mean free path and therefore the total resistivity of the material.

The paper by Bernat, Alexander and Kaae^[2] attempts to make an estimation of the mean free path of the electrons at 4.2 K and find this to approximate 670 nm for 99.99% pure gold. Mean free paths of this order of magnitude are in the range of grain sizes of electrodeposited gold and thus will be an important mechanism for the total resistivity. Matthiessen's rule can thus be expanded to include the resistivity induced by the grain boundaries of an material.

2.2.1.1 Surface scattering

In the previous paragraphs one final scattering mechanism of the conducting electrons is still neglected and this is at the material's surface. When an electron meets the surface of the conducting material it will scatter since it is bound by the material. Normally this effect of the scattering of the conducting electrons can be neglected since it will only occur in samples of thickness comparable to the mean free path. In thin films however, this mechanism can dominate and determine the resistivity. This effect has been studied by Lacey.^[8] The turning point for this effect happens when the electron mean free path l becomes half the size of the layer thickness t . If the electron mean free path l is less than $t/2$ the mean free path of the electrons in the middle of the conducting material will be unaltered and the electrons will not scatter off of the conducting layer surface. The second situation occurs when $l \geq t/2$. In this case the electrons will occasionally scatter off of the conducting layer boundaries and the mean free path of the electrons will be altered, resulting in a higher resistivity.

These two situations are shown in figure 4. In other words, the layer thickness is limiting the mean free path of the conducting electrons if a certain ratio between the layer thickness and the bulk free mean free path is met.

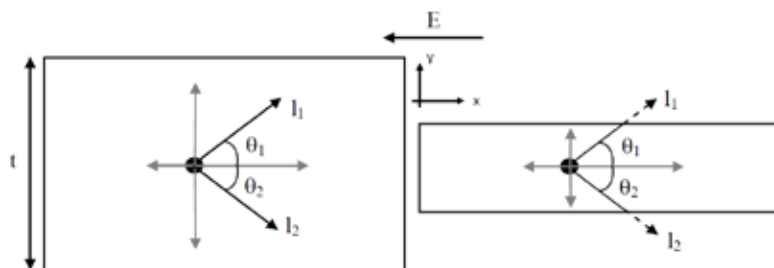


Figure 4: 2-Dimensional structure with electron that a) on the left will not be scattered by the surface b) on the right will be scattered on the surface^[8].

If the approximation of Bernat is taken into consideration as stated in the previous paragraph the electron mean free path of 99.99% pure gold films is around 670 nm at cryogen temperatures. For layer thicknesses in the 1 μm range this effect will become an important factor in the total resistivity of the gold layer at cryogen temperatures.

2.2.2 Metal impurity

The Residual Resistance ratio (RRR) is the ratio between the resistivity of a material at room temperature and the resistivity at 4 K, which can be seen an indication of the purity of an material and can be calculated as followed:

$$RRR = \frac{\rho_{293K}}{\rho_{4K}} \quad [10]$$

where:

- RRR = Residual Resistance Ratio
- P_{293K} = Resistivity at 293 K [$\Omega \cdot \text{m}$]
- P_{4K} = Resistivity at 4 K [$\Omega \cdot \text{m}$]

The bulk room temperature resistivity of gold is listed to be 2.20 $\mu\Omega \cdot \text{cm}$. The RRR values of 99.999% pure gold range from 72 to 280. 99.99% pure gold RRR values ranges from half that of 99.999% pure gold^[4]. Researchers from the Goddard group¹ have achieved RRR values of an electroplated gold layer ranging from 24 to 56 using an 99.9%^[14] pure deposit depending on the gold layer thickness and these values are shown in table 1.^[12]

Table 1: RRR values of electroplated gold layers obtained by NASA's Goddard Space Flight Center ranging from 24 to 56 for various layer thicknesses.^[12]

Layer Thickness (μm)	ρ at 293 K ($\mu\Omega \cdot \text{cm}$)	ρ at 4 K ($\mu\Omega \cdot \text{cm}$)	RRR
0.94	2.90	0.120	24.1
2.0	2.35	0.042	56.3
4.3	2.20	0.049	45.3

¹ NASA's Goddard Space Flight Center is currently the lead developer in cryogenic X-ray thermometers. Their research showed that incorporating gold thermalisation layers with high RRR values greatly increased the performance of their detectors. SRON is aiming to produce gold thermalisation layers with the same RRR values as the Goddard group.

2.4 Electrochemistry of Gold plating

Electrodeposition is often referred to as electroplating or plating in short is an electrochemical technology to protect or enhance a material with a metal coating. The main advantages of electrodeposition over other deposition techniques like vacuum depositions are the lower operating cost, faster deposition rates, the coating of complex shapes, more control and modification of deposit properties and the better control on residual stress of the coating. Vacuum deposition offers lower tolerances, a wider choice of substrates and a wider choice of coatings.

The electroplating process uses an electrical current to reduce the metal ions in a solution to metal atoms on the substrate. The electrical current in the electrolyte is carried by electrically charged ions. Positive ions called cations travel towards the cathode and the negative charged ions called anions travel towards the anode when a potential is applied. Figure 5 shows a schematic

electrochemical cell used for the deposition of gold from a gold sulfate solution. This method uses a reference electrode, working electrode, and counter electrode which in combination are sometimes referred to as a three-electrode setup. In this setup the working electrode is the wafer with the area to be deposited. The combination of the solvent, electrolyte and specific wafer material determines the range of the potential. The counter electrode, also known as the auxiliary or second electrode, can be any material which conducts easily and won't react with the bulk solution. Reactions occurring at the counter electrode surface are unimportant as long as it continues to conduct current well.

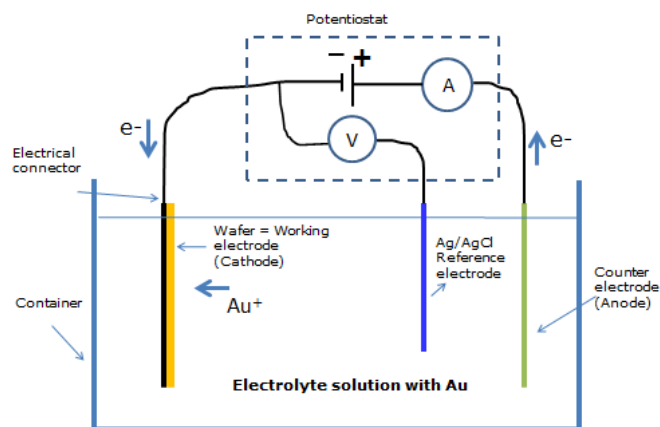


Figure 5: Schematic representation of a electrolyte for deposition of gold from a gold sulfate solution. The working electrode (wafer) is negative. At the cathode the Au^+ to Au reaction takes place, this process gains electrons. The counter electrode (anode) is to conduct the current through the electrolyte.

2.4.1 Electroplating basic principle

When a metal is submerged in an electrolyte that contains its ion and no applied potential is applied, an equilibrium condition is established between the dissolution from and deposition onto substrate. For gold this equilibrium can be expressed as:



However one of the reactions may occur faster than the other resulting in a charge separation. This results in a positively or negatively charged substrate surface and is called the standard electrode potential. Since this is a half-cell reaction, a reference electrode is used to complete the circuit and is given the arbitrary value of zero potential. Using this method the Electro Motive Force (EMF) series was established. the EMF is the voltage developed by any source of electrical energy such as a battery. The origin of this electrode potential was first formulated by W. Nernst and the magnitude of this EMF is given by the Nernst equation:^[9]

$$E = E^0 + \frac{R \cdot T}{n \cdot F} \cdot \ln \frac{a_{\text{products}}}{a_{\text{reactants}}} \quad [12]$$

Where:

E	= Observed EMF	[V]
E^0	= Standard EMF	[V]
R	= Gas constant	[]
n	= Valence change	[]
F	= Faraday's constant	[]
a	= Activity	[]

As a practical approximation the ion concentration can be substituted for the activity of the products and the reactants is the metal solid and it's activity is considered to be 1. If the natural logarithm is converted to logarithm base 10 and the temperature is 298 K then the Nernst equation becomes:^[9]

$$E = E^0 + (0,059/n) \cdot \log(c) \quad [13]$$

where:

c	= Ion concentration	[mol/L]
-----	---------------------	---------

If electrodeposition is to occur an irreversible condition has to be established by overcoming the EMF of the electrode and is done by applying a potential greater than the EMF of the wafer. This potential is called the activation potential.

Faraday's law of electrolysis is the fundamental to electroplating. The quantity of electricity passing through the electrolyte is directly proportional to the amount of chemical change at an wafer.

$$W = I \cdot t \frac{E_q}{F} \quad [14]$$

where:

W	= Weight of deposit	[g]
E_q	= Equivalent weight of deposited element	

The equivalent weight of the element is the atomic weight divided by the valence change (the number of electrons involved). The weight of the deposit is usually converted to the more practical thickness of the deposit. The thickness of the deposited layer can then be calculated using the following formula:

$$d = I \cdot t \frac{E_q}{F \cdot A \cdot \rho} \quad [15]$$

where:

A	= Plating area	[cm ²]
d	= Plated thickness	[cm]
ρ	= Density	[g/cm ³]

The electrochemical processes involved in electrodepositions are far more complex then discussed above and for most electrodepositions the theoretical deposited weight differs from the actual deposited weight. Thus, the efficiency of the electrochemical reaction can be determined as:

$$\eta = 100\% \cdot \frac{\text{actual weight of deposit}}{\text{theoretical weight of deposit}} \quad [16]$$

Polarization or over potential is an influencing factor in the electrodeposition process. A minimum energy is required for any electrochemical reaction to occur. This is the over potential required for the charge transfer reaction and is called the activation over potential. The wafer activation potential shifts the energy level of the ions in the inner electrical double layer nearer to the potential barrier, so that more ions can cross it in a given time, producing a deposit on the wafer surface. Changes in the ion concentration due to the deposition of the ions onto the wafer are a major contribution to polarization and result in changes in the equilibrium potentials as shown in the Nernst equation since the value of $\log(C_E/C_S)$ changes. This effect is called concentration polarization and is mass transport controlled. Increased anode concentration polarization ultimately results in the evolution of oxygen which reacts with the wafer to produce oxide insulating films which increase the ohmic resistance or react with various solution constituents such as organic compounds. Wafer concentration polarization will result in the evolution of hydrogen as the competing reaction and increases the pH of the double layer around the wafer. This raised pH may allow hydrates or hydroxides to precipitate and be occluded into the deposit. Co-deposition of hydrogen may occur as well resulting in impurities and brittleness of the deposit. These effects are unwanted for deposits of high purity and will have to be limited. Figure 6 shows a typical current/potential curve indicating the regions of the activation potential η_a , concentration polarization η_c , limiting current followed by a post limiting current region where gas evolution occurs.^[9]

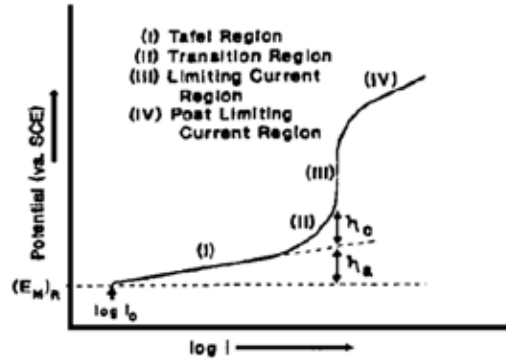


Figure 6: Typical polarization curve^[9]

2.4.2 Bath characterization

Cyclic voltammetry (CV) is most common technique to obtain preliminary information about the electrochemical process. With the help of this method, it is possible to get information about the type of reactions observed in the system and the potentials at which they occur. Standard CV experiments consist of measuring the current flowing through between the Wafer and Counter Electrode as a function of the applied voltage by the Potentiostat. The applied potential is measured against the RE, while the CE closes the electrical circuit for the current to flow. The potentiostat controls the voltage between the RE and WE, while measuring the current through the CE. A typical cyclic voltammogram is shown in figure 7. The voltammetry curve can be used to determine the characteristics of the electrolyte.^[10]

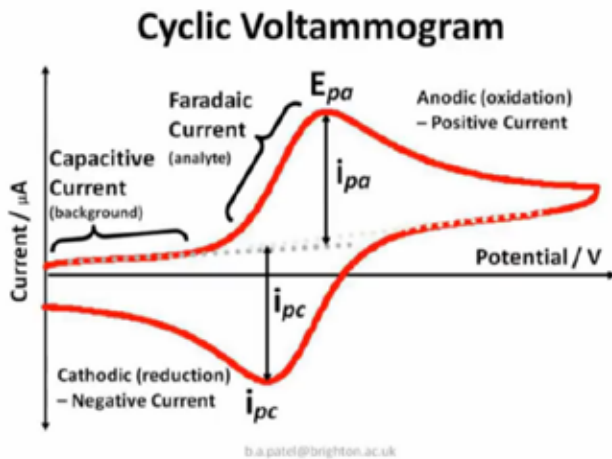


Figure 7: Typical Cyclic Voltammetry (CV) curve.^[10]

2.4.3 Deposition mechanism

If an external potential is applied between the counter electrode and working wafer the ions near the wafer surface rearrange. This creates an electrical double layer called the Helmholtz double layer which is followed by the formation of a diffusion layer as shown in figure 8.

These layers are referred to as the Gouy-Chapman layer. The adsorption process of the metal ions from the bulk of the electrolyte onto the wafer is proceeds as followed:^[9]

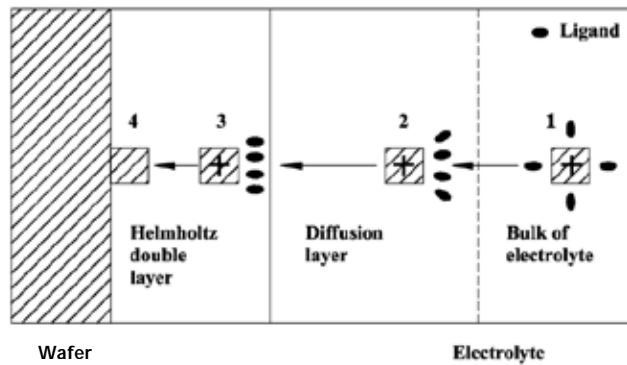


Figure 8: Schematic representation of diffusion layer and Helmholtz double layer close to the wafer surface.^[10]

- Migration: Hydrated metal ions migrate towards the wafer under the influence of an applied electric field as well as by diffusion and convections.
- Electron transfer: At the wafer surface a hydrated metal ion enters the diffusion layer where the water molecules of the hydrated ion are aligned. Then the metal ion enters the Helmholtz double layer where it is deprived of its hydrate envelope.
- The dehydrated ion is neutralized and partially adsorbed on the wafer surface.
- The partially adsorbed atom then migrates or diffuses to the growth point on the wafer surface and is completely adsorbed.

The actual nucleation process is far more complex and described by Paunovic and Schlesinger.^[16] During electrochemical reduction of an ionic species at a wafer as occurs during the process of electrodeposition, the concentration of the reacting species is diminished as a result of this reduction process. The depletion of the reacting species at the surface of the wafer gives rise to a region of non-uniform concentration extending outward from the surface of the wafer until the concentration of the species is that of the bulk of the solution.

The adsorption of the metal ions causes the solution close to the surface to be depleted of ions and this needs to be replenished. This happens through three mechanisms.^[9]

1. The least effective mechanism is ion migration. The migration rate is dependent on the electric field. For some complex ions the migration can actually be in the reverse direction.
2. Convection is the most effective of these mechanisms and involves the movement of the solution. This can be accomplished by mechanically stirring, circulation or air agitation of the solution. The electrodes can be moved through the solution as well.
3. In the close vicinity of the wafer surface diffusion of the ions is the most effective mechanism for ion migration. This diffusion layer is much thicker than the electrical double layer (around 15000 to 200000 times thicker) and depends on the agitation and temperature of the solution. The thickness of this layer is defined as the layer where the concentration of the ions differs 1% from that of the bulk of the solution

If the rate of adsorption of the metal ions onto the wafer surface is limited by the replenishment of the solution close to the wafer surface, the adsorbed metal ions prefer to start new growth sites. The tendency of the adsorbed metal ions to form new growth sites results in small grains. Close to the wafer surface the diffusion of the metal ions is the limiting factor to this replenishment and the rate of diffusion can be increased by raising the thermal energy (temperature of the solution). The agitation of the bath and the temperature both decrease the thickness of the diffusion layer.

2.4.4 Relation microstructure and electroplating operation conditions.

As stated in the paragraph 2.2 the electrical resistivity of a deposited metal is strongly dependent on the grain size and number of impurities. The number of impurities in the deposited metal is a parameter determined by the chemical bath composition. Most commercial plating baths contain additives which are named descriptively. For example, brightener (to give a smooth bright surface finish), levelers, grain-refiners, stress-relievers anti-pitters, etc. Most commercial plating baths are prefabricated baths with these additives and the electrolyte already mixed. To limit the impurities a plating bath without these additives is preferred. Impurities in the deposited metal could also occur from contamination of the plating bath. It is nearly impossible to maintain a plating solution free of these contaminations. Some common of potential contamination sources include:^[9]

1. Chemicals used to for maintenance of the bath
2. Impure anode
3. Improperly cleaned anodes
4. Decomposition of addition agents
5. Improper rinsing and drag in of solution from previous steps
6. Fall in from airborne dirt, oil or other particles
7. Chemicals in water used for volume replenishment

The size of the grains in the deposited metal is dependent on a number of factors and some of these factors are easily controlled plating conditions.^[13] And overview these of the plating conditions and their effects on the grain size is shown in figure 9. The metal ion concentration and addition agents are given bath compositions. Current density, bath temperature, bath agitation and polarization are properties which are controllable during the deposition runs. The optimal plating conditions need to be established empirically. The different influences are all related and it is impossible to select the optimal plating conditions based solely on the theory.

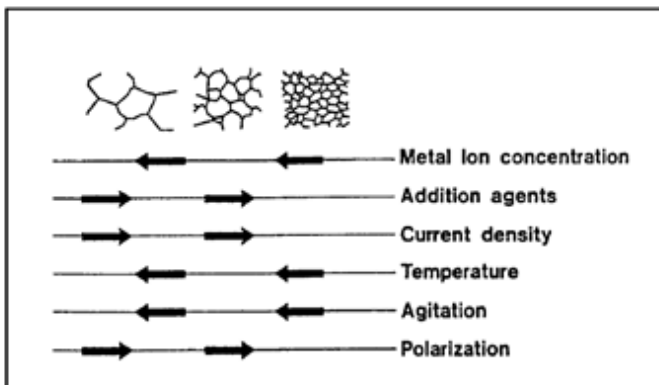


Figure 9: Relationships between the grain size of electroplated metal and the plating conditions.^[13]

- **Gold ion concentration**
The concentration of the gold ions has a direct effect on the number of adsorbed ions onto the wafer surface. Higher concentrations of gold ions allow for more reductions onto the wafer surface allowing the crystal structures to grow faster resulting in larger grains.
- **Addition agents**
Addition agents are foreign ions in the electrolyte which are added for different purposes. Brightener for instance is added to give a bright and smooth surface finish. The brightener ions are adsorbed onto the wafer surface and provide extra growth points for the gold ions. More growth points result in smaller grain sizes since more individual crystallites are able to form. Additives are a source of impurities as well since additional ions are adsorbed onto the wafer surface.
- **Current density**
A lower current density will allow the gold ion to migrate on the wafer surface for a longer period of time giving them more time to migrate into a growth point. Higher current densities will adsorb the ions faster and won't allow all the ions to migrate into a growth point and new growth points will be created. More growth points will result in small grains since more crystals will form.
- **Bath temperature**
The tendency of the deposited gold ions to form new growth sites has a relation with the replenishment of the ions close to the wafer surface. A higher bath temperature or more thermal energy of the gold ions increases their diffusion rate. As discussed in the previous paragraph the diffusion rate is the limiting factor on the replenishment of the gold ions close to the wafer surface and thus a high diffusion rate will favor the tendency of the gold ions to grow on existing crystals resulting in larger grains.
- **Bath agitation**
Bath agitation has an effect on the size of the diffusion layer. By mechanically stirring the bath the concentration of the gold ions in the bulk of the solution will be increased externally allowing the gold ions to move closer to the wafer surface. The bath agitation thus has an effect on the replenishment of the gold ions close to the wafer surface just like the bath temperature. Proper bath agitation will thus cause larger grains to grow.
- **Polarization**
An too high over potential causes several detrimental effects on the purity of the deposited layer. These impurities provide extra nucleation points for new grains to grow. Several of the other steps available to increase grain sizes have an effect on the polarization as well. Staying in the activation polarization region as shown in figure 6 will eliminate the concentration polarization. This can be achieved by lowering the over potential in the electrochemical cell and is related to the current density. Selecting a low current density range will result in less polarization and will result in larger grains

3 Experimental setup

This chapter will give an overview of the experimental setup used at SRON for electroplating the gold microfilms. The necessary steps for the production and characterization of the electroplated gold structure will be discussed.

3.1 Electroplating setup

3.1.1 Electrolyte

The electroplating bath (electrolyte) used for the electroplating experiments is a commercially available electrolyte called NB SEMIPLATE AU 100. This is an alkaline, sulfite based electroplating formulation supplied by Microchemicals and produces a bright, ductile deposit. As stated in the technical data sheet the NB SEMIPLATE AU 100 electrolyte demonstrates exceptional throwing power that results in good coverage of recesses, holes and hollows of parts of complex geometry. The NB SEMIPLATE AU 100 electrolyte is also easy to use, less toxic than cyanide electrolytes and very stable. The electrolyte comes in prefabricated mixtures for optimal concentrations of all the additives and separate mixtures to be fabricated on site. Table 2 shows the composition of the Au-sulfite plating bath and the optimal operating conditions. The entire datasheet is found in Appendix C.

Table 2: Physical properties of the electrolyte, optimal plating conditions and the specific procedures of the NB semiplate AU 100

Physical properties of the deposit	
Au-sulfite electrolyte	
purity	99.9%
pH	± 9.5
Optimal Plating conditions	
Cathode Current density (mA/cm ²)	1.5
Anode-Cathode spacing (cm)	5-15
Electrolyte temperature (°C)	30
Specific Procedures	
Oxygen plasma before plating	

3.1.2 Power source

The power source is from MetroOhm. The Autolab PGSTAT204 is a compact and modular potentiostat/galvanostat with a compliance voltage of 20 V and a maximum current of 400 mA. The Autolab can be placed anywhere in the lab and is easily controlled with the provided NOVA software and can be used for most of the standard electrochemical techniques. The technical details of the Autolab PGSTAT204 can be found in Appendix D. This power source is controlled through software provided by the manufacturer and is called NOVA. This program allows the user to build the most complex of electrical signals through the electrochemical cell.

The entire electrochemical cell was positioned on top of a hot-plate magnetic stirrer to provide the bath agitation and control the temperature of the electrolyte. Figure 10 shows a photo of the entire electroplating setup.

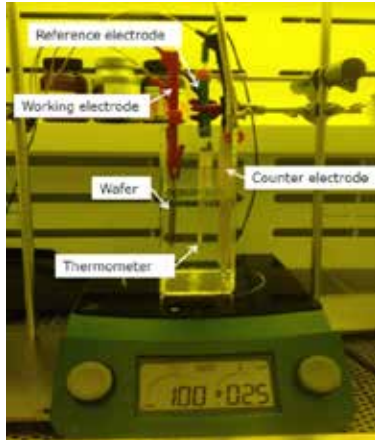


Figure 10: Photos of experimental electroplating setup. On the left the electrochemical cell with the wafer. On the right the PGSTAT204 connected to a laptop running NOVA

3.1.3 Wafer preparation

Figure 11 shows the steps performed to obtain the measurable electroplated test structure. The process starts with the evaporation of 15/65 nm Titanium/Gold plating base (seed layer) on a Si_2N_4 coated Si wafer with a 4 inch diameter. This wafer is then coated using AZ6612 photo resist. Squares areas of resist were exposed with UV light and developed resulting in a 1 cm^2 area of exposed seed layer as shown in in figure 12

Before the electroplating, wetting of the exposed area on the wafer was improved by applying an oxygen plasma to remove organic contaminations on the plating base surface. After the wetting improvement the wafer is emerged in the electrolyte and the deposition run is started. A schematic front view of the wafer submerged into the electrolyte is shown in figure 12. An area of 1 cm^2 was chosen for deposition so that the current density was easy to calculate. The plating condition will be varied to establish the optimal settings. After the deposition run the resist layer is stripped by submerging the wafer in acetone. A new photo resist layer will be applied and a test structure patterned. The electroplated gold layer and the Ti/Au seed layer are then etched using the remaining resist as mask, resulting in a free standing test structure. Finally the photoresist is stripped and a clean test structure is ready for testing. Detailed information of these deposition steps can be found in the LOT traveler in appendix E.

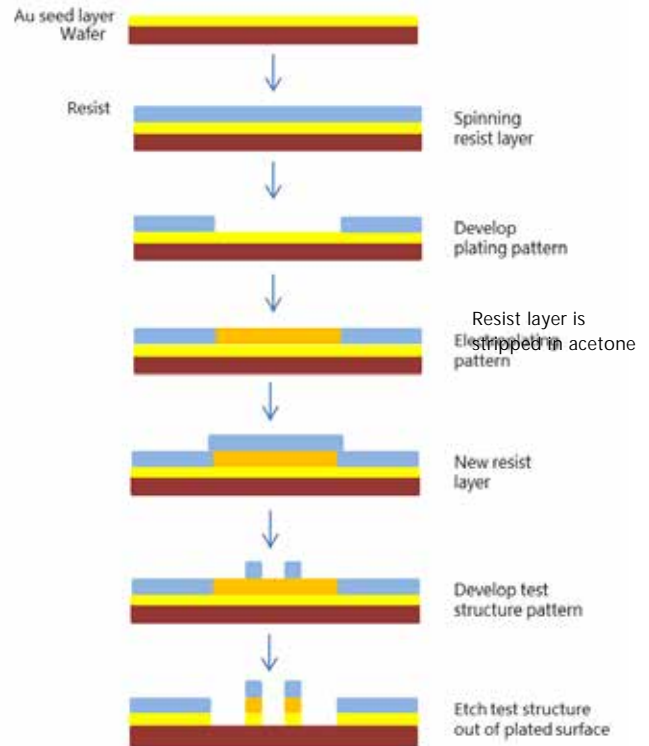
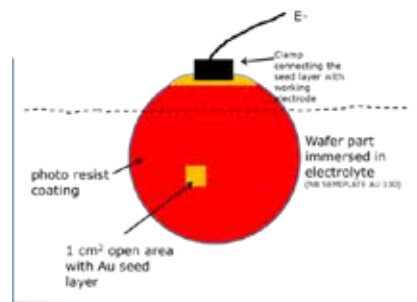


Figure 11: Schematic representation of the steps performed to obtain electroplated test structures.

Figure 12: Schematic front view of wafer in submerged into the electrolyte. Area of 1 cm^2 is exposed to solution.



3.2 Diagnostic tools

3.2.1 Resistance measurements at room temperature

In order to measure the resistance of the deposited gold film the plated area has to be etched into a measurable structure. For this we made use of the so called "Hall bar" geometry, shown in figure 13.



Figure 13: Hall Bar structure for four point probe resistance measurements of a electroplated gold layer.

The dimensions of a Hall bar structure are such that a four point probe resistance measurement can be performed. By applying a current on two of these contact pads and measuring the voltage drop over the remaining two contact pads the resistance of the metal connecting path is measured. Using this method the contact resistance is eliminated from the measurement. The measured metal film is 40 μm wide and 4000 μm long resulting in 100 squares. If the thickness of the gold film is known the resistivity (ρ) of the deposited gold can be calculated.

The seed layer on the wafer of 16 nm Titanium and 65 nm gold has a set resistance and the measured resistance will be corrected by treating this seed layer as an parallel resistance. The influence of the seed layer will be layer thickness dependent. By correcting the resistance of the structure for the seed layer the resistance of the actual deposited layer is obtained. The thickness of the structures is measured using an DEKTAK surface profiler. Using the measured resistance and thickness of the structures the resistivity of the deposited structures can be calculated. The surface roughness can be measured using the DETKTAK surface profiler in the nanometer scale.

3.2.2 Resistance measurements at 4 kelvin

To measure the resistivity at cryogen temperature the test structures need to be cooled to 4K. This is achieved by dipping them into liquid helium. Only small chips fit onto the sample holder, so this the wafer has to be diced using a diamond tip cutter. The individual chips are then mounted onto a printed circuit board (PCB) and wire bonded using aluminum wires. These PCB's are then mounted onto the dipstick which is shown in figure 14. For each deposition run 2 Hall bar structures were etched into the deposited layer and are wire bonded to the PCB. Each structure uses 4 channels to measure the resistance of the deposited gold and so 8 channels are used per PCB. The dipstick has 24 channels which can be connected during 1 cooling run and so 3 PCB with 3 different deposition runs can be cooled at the same time.



Figure 14: Photo of dipstick used to dip test structures into liquid helium.

The dipstick with the mounted test structures is then inserted into the helium tank. The tip of the dipstick is then lowered down into the liquid helium and thus cooled to 4 K and measured using an AVS-47 resistance bridge. Figure 15 shows a photo of the dipstick tip after dipping the structures into liquid helium.

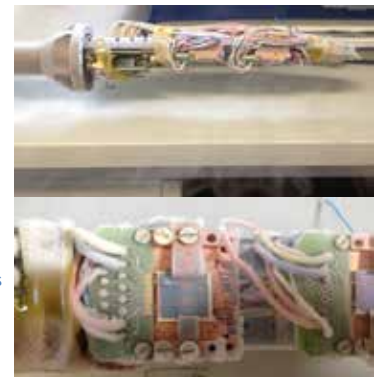


Figure 15: Photo of dipstick with mounted structures after dipping in liquid helium for resistance measurements at 4 K

3.2.3 Microscopic inspection

The deposited surfaces and etched structures were analyzed under an optical microscope (figure 16) and using a Scanning Electron Microscope (SEM) (figure 17). The surface can be observed closely using these methods. The structures are first analyzed under an bright field optical microscope. As discussed in paragraph 3.1.3 the etching of the structure resulted in the edge of the test structures to be exposed to the etching chemicals for some time. The actual width of the Hall bar might be less than the designed width of 40 μm due to under etching. So to be able to determine the resistivity of the deposited gold layer the width of the Hall bar structure had to be measured. This was done using the optical microscope. Top view photos of the structures were taken and then the width of the structures was obtained by measuring the structures. Using a differential interference contrast technique on the microscope more information on the surface finish of the deposited gold layers can be obtained.

Higher magnification photos of the deposited gold layer surfaces are obtained using an SEM. Using the SEM the individual grains of the deposited gold layers can be visualized and their size can be estimated.



Figure 17: Photo of Bright field optical microscope

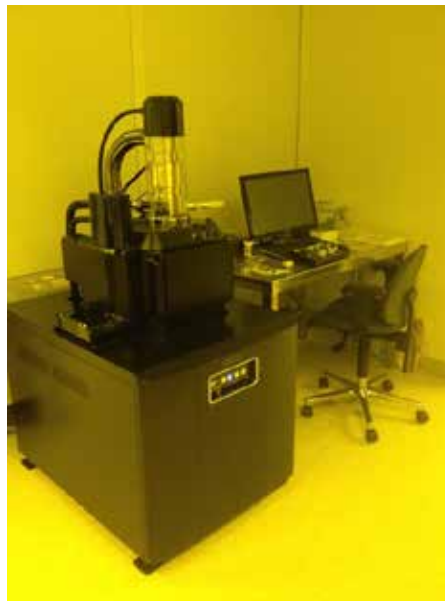


Figure 16: Photo of Surface scanning Electron Microscope (SEM)

4 Experimental results

First the bath characterization is conducted by performing a Cyclic Voltammetry (CV) to obtain the potential region in which deposition of gold onto the electrode is conducted. Then the amount of bath agitation through mechanically stirring the solution is obtained. The last characterization is the use of a current- or potential biased power source. After obtaining stable deposition settings the plating conditions can be varied to optimize the setup.

The effect of bath temperature and current density is then determined. This is done by a number of deposition runs under different bath temperatures and current densities. The deposited layers are kept in the 500 nm range to be more time efficient. Deposited layers are analyzed using the optical microscope and by analyzing the room temperature resistivity. From these test structures an optimal region for deposition is obtained and layers ranging from 1 to 4.5 μm are fabricated. Not all fabricated structures could be cooled since this is a time consuming process so a selection has been made. These thicker layers are cooled to 4 K and the cryogenic resistivity is obtained. Using this the RRR value of these deposited gold layers is calculated.

Using the previously obtained optimal range for depositing gold layers with the best cryogenic resistivity an deposition runs is done using a different electrolyte. This electrolyte is without the addition agent brightener and should result in deposited layers with larger grains.

4.1 Bath characterization

4.1.1 Voltammetry curve

Using the Cyclic Voltammetry program provided in the NOVA software of the Autolab PGSTAT 204 an voltammetry curve of the electrolyte is obtained. This program scans the potential and measures the current flowing through the electrolyte. It starts at a potential of 0.0 V and is increased to 0.5 V with steps of 2.4 mV. When the potential reaches 0.5 V the steps are reversed and the potential is brought down to -0.8 V and then increased to 0.0 V again. This cycle is repeated 10 times. The program is shown in figure 18. The resulting voltammetry curve is shown in figure 19. In this curve the cathodic current and the start of the anodic current are shown. The cathodic peak is shown at -0.7 V. The reduction of gold ions onto the wafer surface occurs in this region.

Commands	Parameters	Links
Marcel R WITH OCP		
Remarks	Cyclic voltammetry pote...	...
End status	Autolab	...
Signal sampler	Time, WE(1).Potential...	...
Options	1 Options	...
Instrument		
Instrument description		
Autolab control		...
OCP determination	[0.000]	
Set reference potential	0.000	
Set potential	0.000	
Set cell	On	...
WE(1).Cell	On	...
Optimize current range	5	
CV staircase	[0.000, 0.500, -0.800, 0.00...	
Start potential (V)	0.000	
Upper vertex poten...	0.500	
Lower vertex poten...	-0.800	
Stop potential (V)	0.000	
Number of stop cro...	10	
Step potential (V)	-0.00244	
Scan rate (V/s)	0.1000000	

Figure 18: Program used to obtain the voltammetry curve

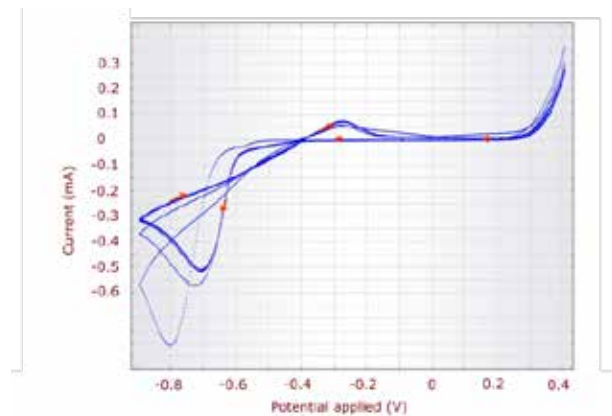


Figure 19: Voltammetry curve obtained using the program shown in figure 17

4.1.2 Bath agitation

Multiple electroplating runs were conducted to determine the influence of the bath agitation on the deposition mechanism. Ideally the plating conditions are identical for the entire area of the wafer at which the adsorption of the metal ions occur so that a perfectly homogenous microfilm can be produced.

By mechanically stirring the solution the concentration of the gold ions in the bulk of the solution will be increased allowing the gold ions to move closer to the wafer surface. Without proper bath agitation the reactions are limited by the diffusion of the solute gold ions. The diffusion of these ions happens at random and therefore not only greatly decreases the plating rate but the homogeneity of the deposited gold film and greatly increases the number of grain boundaries. Ideally the bath is agitated in a way that the adsorption of gold ions onto the substrate is no longer limited by the diffusion of gold ions but by the applied voltage over the anode and cathode. To demonstrate this dependency of the deposition speed the following experiment was conducted. During the deposition of gold onto the substrate the agitation of the bath was realized by stirring the solution. The deposition of gold was started without any form of bath agitation. By doing so the deposition rate was allowed to be limited by diffusion. After 60 seconds of deposition the agitation was started and increased with steps of 10 rpm every 10 seconds. This was done for different applied voltages ranging from -0.5 V to -0.65 V with the electrolyte at 20 degrees Celsius. The results of these test are show in figure 20.

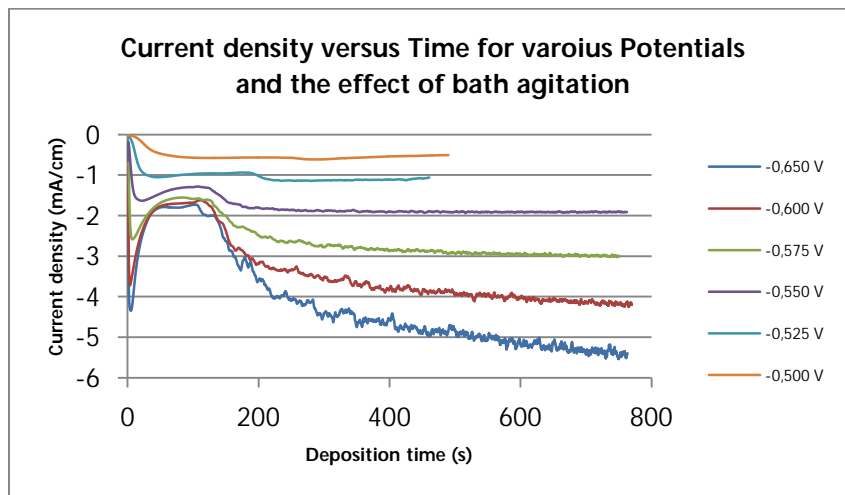


Figure 20: Current density versus time. Higher applied voltages have an increased effect from bath agitation.

The current doesn't rise immediately after the agitation of the bath has started and is due to the inertia of the bath. The bath needs some time to start a constant flow. Therefore the second step was applied 30 seconds after the first step. The graph shows a number of things.

First the effects of the bath agitation, the faster the bath is stirred the lower the current drops. After the stirring speed is increased to around 400 rpm the current reaches a lower limit for the applied voltages of -0.5 V to -0.575 V. In this region the reaction rates at the wafer surface isn't limited by the diffusion rate any more.

The bath agitation has the most effect on the higher current densities. This can be explained by the rate at which the gold ion adsorption takes place. Without the bath agitation the diffusion of the gold ions is the limiting factor for the adsorption rate and is current density independent. For the higher applied voltages and thus higher current densities the adsorption rate is raised a considerable amount by the bath agitation, however these higher current densities have considerable more variation. This could be explained by local variations of the flow of the electrolyte around the wafer surface. The stirring of the bath was selected to be 500 rpm for the following experiments.

4.1.3 Voltage bias versus current bias

The experimental electroplating setup can be operated using two different settings. The Amperometry allows the user to set a potential and the software will regulate the current flowing through the electrolyte to maintain a user defined potential. The Potentiometry allows the user to set a current and the software will regulate the potential to maintain the set current. The first test were conducted using the Amperometry and thus a set potential. After optical microscope inspection of the deposited gold layers the surface showed some inhomogeneity. The thickness showed to vary slightly across the deposited surface and the resistivity was very inconsistent. The structures deposited using the Potentiometry showed to be much more reproducible resistivity and thickness of the deposited gold layers. The resistivity of these tests are shown in figure 21.

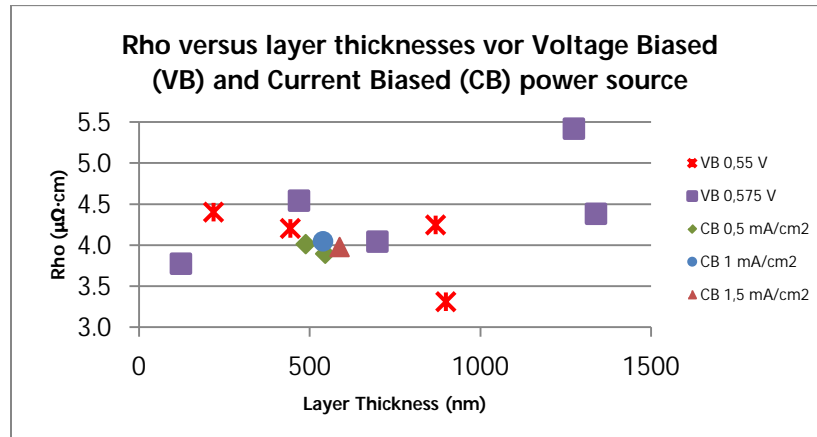


Figure 21: Resistivity of deposited test structures versus layer thickness for an current and voltage biased power source.

Switching the power source from voltage biased to current biased also greatly improved the consistency of the plating rate which can be found in Appendix F resulting in reproducible layer thicknesses. Based on these results the Potentiometry was used as a default for further testing.

4.2 Comparison of various plating conditions

The datasheet of the NB Semiplat AU 100 states that the nominal bath temperature is at 30 degrees Celsius and the optimal current density is at 1.5 mA/cm². From theory stated in chapter 2.4.4 we assume that the grain sizes would increase with lower current densities and higher bath temperatures. To assess the effect of these parameters the current density was varied from 0.25 mA/cm² to 2 mA/cm². The bath temperature was varied from 20 degrees Celsius to 60 degrees Celsius. Table 3 shows the different plating conditions used to analyze the effect of current density and bath temperature on the resistivity of the deposited gold layer.

Table 3: Overview of the varied plating conditions used to study the resistivity of the deposited gold layers.

I (mA/cm ²)	Bath Temperature (C)
0.25	20,30,40,50 and 60
0.5	20,30,40,50 and 60
1	20,30,40,50 and 60
1.5	20,30,40,50 and 60
2	20,30,40,50 and 60

4.2.1 Effect of current density

The deposition runs were executed using the plating conditions shown in table 3 and the previously obtained bath agitation of 500 rpm and the Potentiometry for reproducible deposition layers. The resulting resistivity of these test structures are shown in figure 22. This figure shows the influence of the current density for each bath temperature.

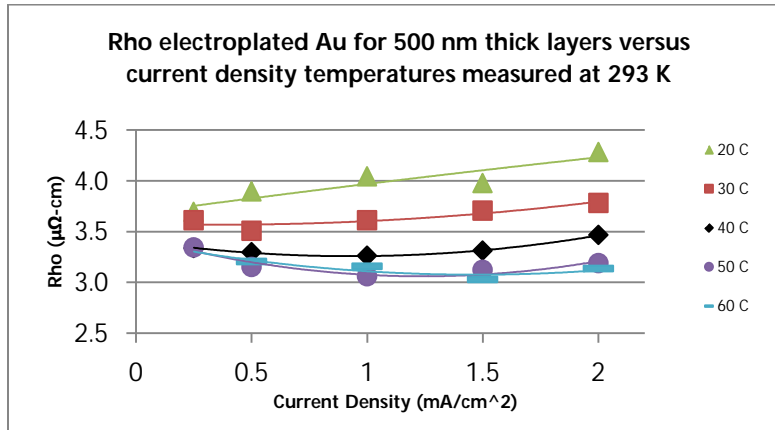


Figure 22: Rho of electroplated test structure vs current density for different bath temperatures.

First let's examine the green trend (bath temperature at 20 degrees Celsius). The current density behaves just as the literature describes. The increasing current density lead to smaller grains and thus increases the resistivity of the deposited gold layers.

The next trend is the red curve (bath temperature at 30 degrees Celsius). This trend behaves like the literature as well showing an increase in resistivity with increasing current density. One thing does stand out in this trend and that is that at a current density of 0.5 mA/cm² the trend shows a minimal value for the resistivity.

The trends at 40, 50 and 60 degrees Celsius show the same effect as the trend for the resistivity at 30 degrees Celsius. The minimal value for the resistivity shifts to higher current densities as the bath temperature rises. We assume that at higher bath temperatures in combination with current densities lower than 1 mA/cm² other mechanism become more dominant in the process of grain formation. Additives could be involved in these mechanisms.

4.2.2 Effect of bath temperature

To better understand the effect of the bath temperature the same deposited test structures as in figure 21 are shown using the bath temperature as the x-axis and is shown figure 23.

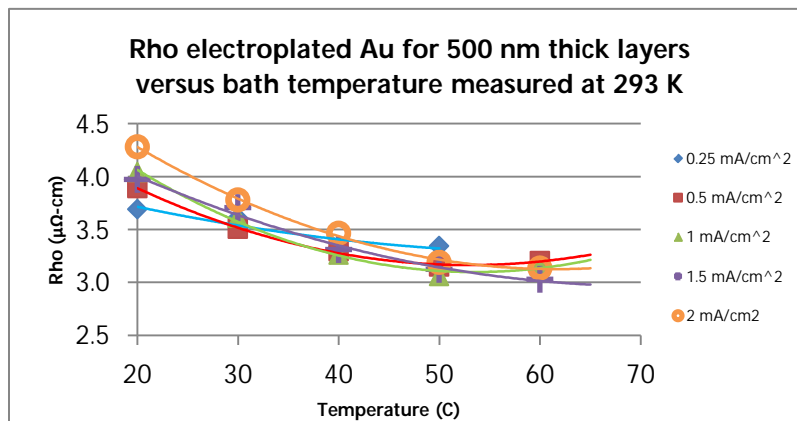


Figure 23: Rho of electroplated test structures versus bath temperature for different current densities.

Let's examine the first trend (blue trend at 0.25 mA/cm^2) again. This trend shows an almost linear decrease of the resistivity of the deposited layers with increasing bath temperature as to be expected from the literature.

The next trend for the current density at 0.5 mA/cm^2 starts with a higher resistivity with the bath at room temperature but decreases more rapidly as a function of the bath temperature. This trend has a minimum at around 50 degrees Celsius.

The trends for the current densities at 1.0 and 1.5 mA/cm^2 show the same effect as the trend for the current density at 0.5 mA/cm^2 . Both start an increased resistivity with the plating bath at room temperature and decreases with increasing bath temperature. The minimum for the current density at 1.0 mA/cm^2 occurs at the same temperature as the trend for the current density at 0.5 mA/cm^2 . The trend for the current density at 1.5 mA/cm^2 shows a minimum at 60 degrees Celsius. Both minimums have a bottom value of $3.0 \mu\Omega\text{-cm}$.

The last trend shows the same trend as well. The start of the trend is even higher than the previous trends and drops down fast with an increasing bath temperature. This current density has the greatest effect on the resistivity from the increased bath temperature. However the minimum has shifted upwards and the trend reaches a minimum of around $3.20 \mu\Omega\text{-cm}$ just like the current density at 0.5 mA/cm^2 .

Varying the bath temperature resulted in an overall lower resistivity but dependent on the applied current density. An optimal region has been established for further investigation. To obtain more information on the influence of the layer thickness the current density of 1.0 mA/cm^2 and the bath temperature at 50 degrees Celsius were selected to deposit the next test structures.

4.2.3 Microscopic examination:

Figure 24 and 25 show photos taken under an optical microscope and SEM of the selected test structures surfaces. A smooth and bright gold color is observed. Micrographs under the SEM show small pits and bumps but these have sub-micron dimensions. No grains are visible under the optical microscope and even the SEM indicating very small grain sizes. The darker colored areas are surface roughness effects which have thicknesses in the nanometer range. Note that the edges of the test structures are rough and this is a byproduct of the etching steps of the Hall bar pattern. These have a small effect on the thickness and thus the geometry of these structures.



Figure 24: Electroplated test structure as seen under an optical microscope.

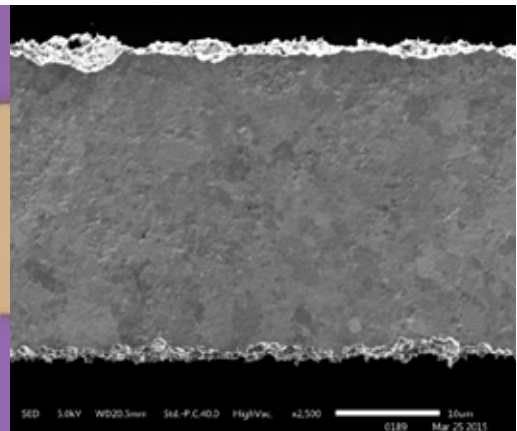


Figure 25: SEM micrograph of the same test structure. The Bar shown is $10 \mu\text{m}$ long

4.2 Effect of layer thickness on the resistivity

The previous obtained test structures were deposited with a layer thickness of 500 nm to limit the production time. In order to compare the RRR values with the values obtained by the Goddard group thicker layers had to be deposited. The thicknesses deposited by the Goddard group are 1, 2 and 4.3 μm and we aim to reproduce these layer thicknesses. The optimal electroplating conditions established in the previous tests were maintained for these thicker test structures. A stirring speed of 500 rpm, a current density of 1 mA/cm^2 , bath temperature at 50 degrees Celsius and the Potentiometry power source. A second 1 μm layer was deposited using the same conditions except for the bath temperature which was raised to 60 degrees Celsius. The resistivity of these layers deposited using these plating conditions is shown in figure 26.

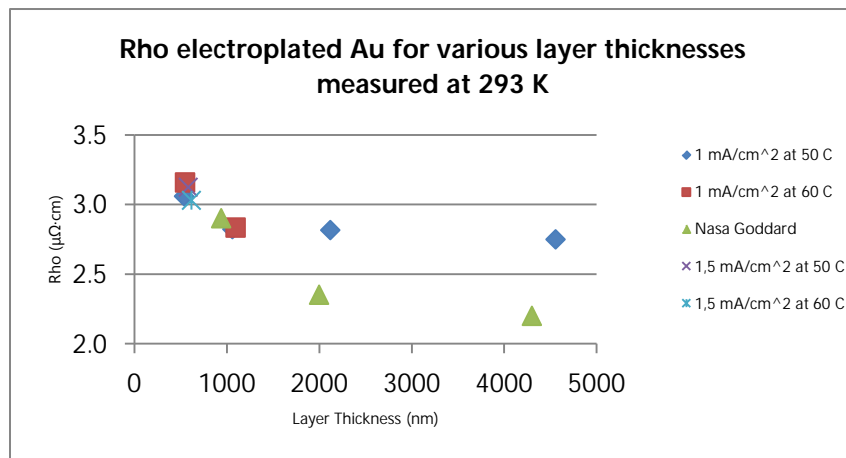


Figure 26: Resistivity of electroplated test structures versus layer thickness for different current densities and bath temperatures. NASA's obtained room temperature resistivity is given as comparisons.

Results for the thinner layers of 500 nm are given as well. The thinner layers have a room temperature resistivity which is comparable to those of the Goddard group, although higher than the bulk value. The thicker layers of 2.3 and 4.6 μm are considerably higher than expected. These should drop as a function of the layer thickness. This could be an indication that the grain sizes are still limiting the conduction of the electrons. Goddard's room temperature resistivity are shown and for its thickest layer reaches the bulk value of $2.20 \mu\Omega\cdot\text{cm}$.

4.2.4 Measuring RRR values

Several samples were mounted and cooled to 4.2 K by dipping them in liquid He. Results are shown in figures 27 and 28. Plating conditions are indicated

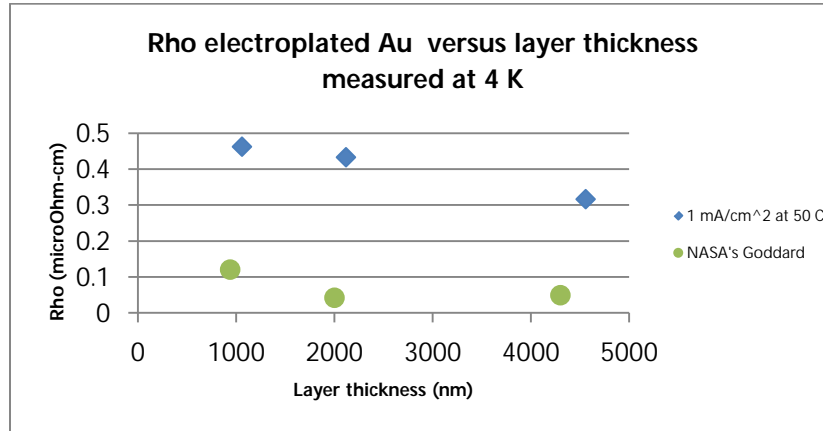


Figure 27: Resistivity of selected structures at cryogen temperature.

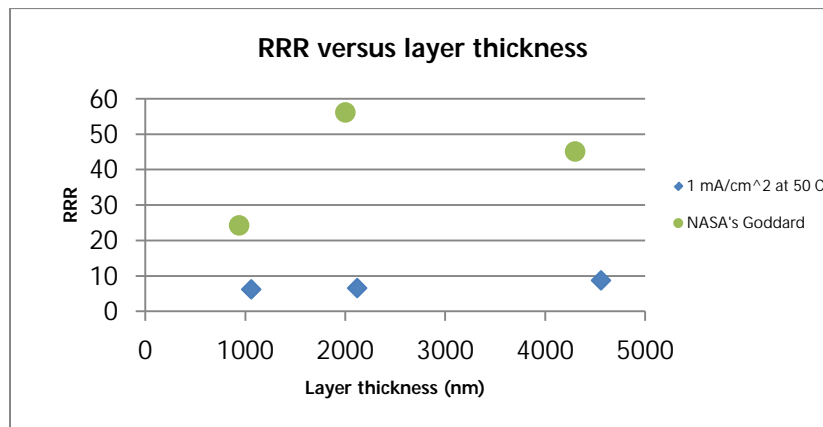


Figure 28: RRR of selected structures deposited under previously optimal conditions.

The resistivity at 4 K of the deposited layers ranged from 0.46 $\mu\Omega\cdot\text{cm}$ to 0.31 $\mu\Omega\cdot\text{cm}$. These measured resistivity's resulted in RRR values between 6 and 9 and more optimization is required to further increase the cryogenic resistivity and RRR of the deposited gold layers. An electrolyte without the brightener additive was purchased in an attempt for further optimization.

4.5 Effect of Brightener

To further improve the resistivity and the RRR value of the deposited gold layers the remaining electroplating parameters have to be analyzed. The effect of brightener is one of these and the electrolyte without this brightener was purchased. Some first tests have been conducted with this new electrolyte and these are showing positive results. These were conducted using the optimal plating conditions established for the electrolyte with brightener. A first test run was done with and bath agitation by mechanically stirring at 500 rpm, a current density of 1 mA/cm^2 , the electroplating bath at a temperature of 50 degrees Celsius and the Potentiometry power source. These resulted in the room temperature resistivity's seen in figure 29.

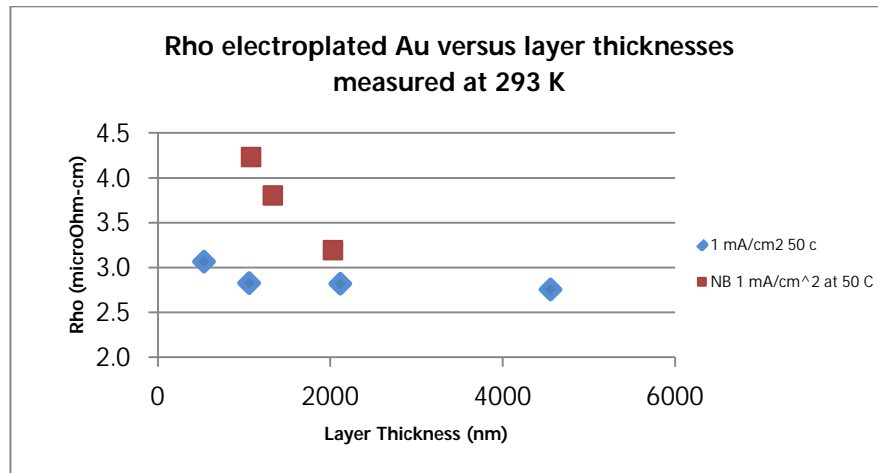


Figure 29: Room temperature resistivity's of deposited gold layers using an electrolyte with brightener and No Brightener (NB).

The room temperature resistivity increased considerably. During the deposition run a current of 1 mA/cm^2 was maintained and an higher voltage than during the deposition runs with an electrolyte with brightener was observed. This could indicate a different behavior of the electrolyte without brightener. The deposited gold layers were observed to not be bright gold colored. The surface appeared to be rough as seen under the naked eye. Optical inspection of the deposited layer using the electrolyte without brightener showed some remarkable structures and are shown in figure 30.

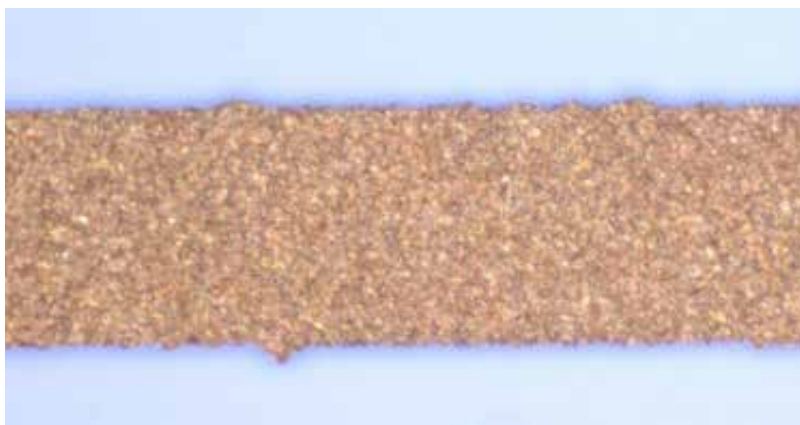


Figure 30: Photo of deposited gold layers surface using an electrolyte whiteout brightener.

The surface of the deposited layer as seen under an optical microscope shows different colored dots. These could be the individual grains and this layer was further analyzed using the SEM. The photos taken using the SEM are shown in figure 31.

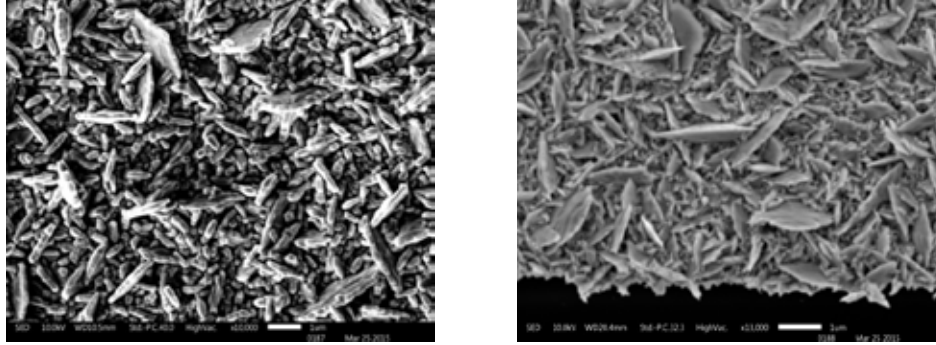


Figure 31: Deposited gold structures using an electrolyte without brightener showing individual crystals randomly orientated. Left and right micrographs are obtained using different SEM settings.

The SEM micrographs show large crystalline structures with a size of a couple hundred of nanometers thick and 1 μm long with sharp edges. The effect of the brightener is clearly visible when these micrographs are compared to the micrograph taken of the deposited layers with brightener in the electrolyte shown in figure 25. A very rough surface finish is not preferred as this will increase resistivity through surface scattering. The deposited structures using the electrolyte without the brightener were cooled to 4 K by dipping them into liquid helium and the resistivity was measured and resulted in the resistivity's shown in figure 32. The corresponding RRR is shown in figure 33.

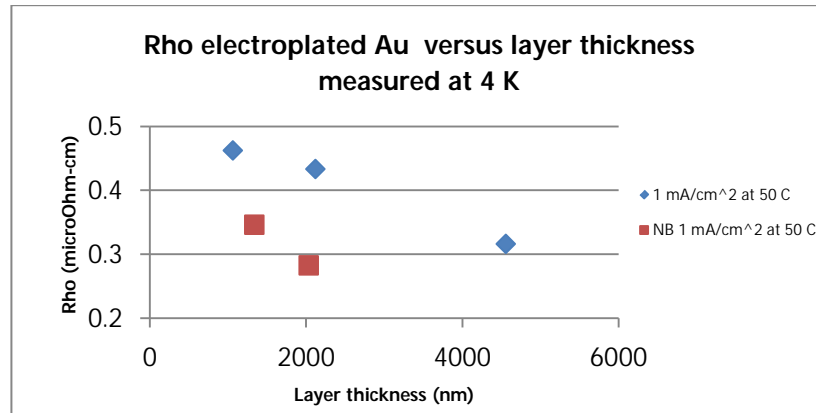


Figure 32: Resistivity's of selected gold structures measured at cryogen temperature.

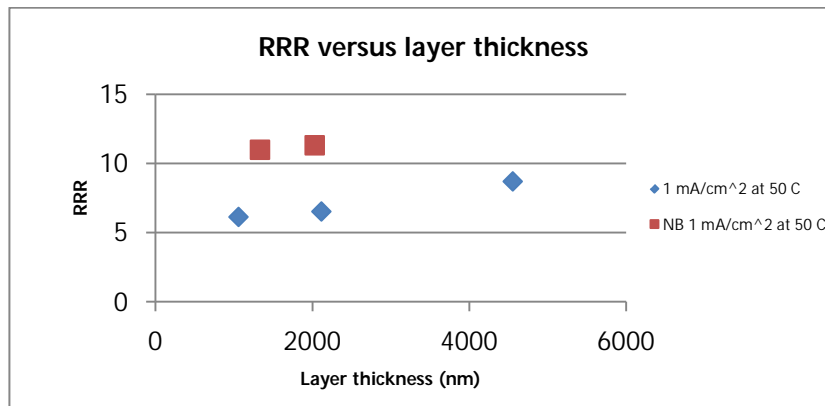


Figure 33: RRR of deposited gold structures under the optimal conditions.

The cryogenic resistivity of the gold structures deposited using the electrolyte without the brightener has halved in comparison to the cryogenic resistivity of the gold structures using the electrolyte with brightener. The resulting RRR increased to 11 for both layer thicknesses. The rise of the RRR is mainly from the higher room temperature resistivity. In these layers the surface scattering will most likely be the limiting factor of the mean free path of the conducting electrons. The size of the grains has greatly improved from using an electrolyte without brightener.

5 Discussion

In this chapter the observed cryogenic resistivity's will be discussed and an attempt to find the limiting factor on this resistivity. The observed residual resistivity was observed to be higher than obtained by Bernat^[2] and the Goddard group. The resistivity at cryogenic temperature and RRR observed and the values found in the literature are summed up in table 4.

Table 4: Overview of the observed resistivity at cryogenic temperature and RRR and the resistivity at cryogenic temperature and RRR found in the literature (* electrolyte without brightener).

Layer Thickness (μm)	SRON		Goddard ^[12]		Bernat ^[2]
	RRR	ρ at 4 K ($\mu\Omega\cdot\text{cm}$)	RRR	ρ at 4 K ($\mu\Omega\cdot\text{cm}$)	RRR
0.94	6	0.46	24	0.12	24-35 (RRR values not related to layer thicknesses)
1.4	11	0.35*	-	-	
2.0	11	0.32*	56	0.04	
4.3	9	0.32	45	0.05	

Our approach in finding the limiting factor on the cryogenic resistivity is as followed. First off the purity of the deposited gold layer is compared to the purity of the gold layers deposited by Bernat and the Goddard group. Next the effect of surface scattering on the residual resistivity is analyzed by estimating the mean free path of the conduction electrons. Finally the grain size will be estimated based on the RRR and residual resistivity. This estimation will be validated using the SEM micrographs.

5.1 Deposition purity

The used electrolyte (NB Semiplat AU 100) is listed to produce an 99.9% pure gold deposit. Purities of 99.99% result in an RRR ranging half that of 99.999% pure gold^[2]. A purity of 99.9% will have an even lower range of RRR indicating that purities will limit the resistivity at some point. A small variation in purity can thus be a huge influence on the RRR and therefore the residual resistivity. Table 5 shows an overview of the purity of the deposited layers of Bernat and the Goddard group and their respective RRR. Higher purities with their respective RRR range are shown as well.

Table 5: Overview of the different purities of deposited gold and their respective RRR

Purity (%)	RRR
99.9	5- 35 (Bernat ^[2]) 24-56 (Goddard ^[12]) ²
99.99	72 - 140 ^[2]
99.999	Up to 280 ^[2]

The purities of the deposited gold layers from Bernat and the Goddard group are found to be 99.9% from this we assume that the deposited gold layer residual resistivity *is not limited by purity*. The purity certainly ensures a lower limit of the residual resistivity but with the current deposited gold layers this lower limit is not yet met. Residual resistivity of the desired values should be achievable using the current electrolyte.

² For purity the datasheet of Techni Gold refers to Type III A of MIL-G-45204 C (ASTM B488-95 as revised). According to this specification this means a purity of 99.9 percent gold minimum.

5.2 Estimated mean free path.

For further discussion of the effect of surface scattering and grain boundary scattering an estimation of the mean free path is required. The relation between the mean free path of the electrons and the residual resistivity is described by Brown^[3].

$$l = \frac{(r_s/a_0)^2 \cdot 9.2 \text{ nm}}{\rho} \quad [17]$$

where:

l	= Mean free path	[nm]
r_s	= Radius of the free electron sphere	[]
ρ	= Residual resistivity	[$\mu\Omega\cdot\text{cm}$]
a_0	= Bohr radius	[]

using this relation they found an mean free path of 2 micron for samples with an residual resistivity of $0.04\mu\Omega\cdot\text{cm}$. based on these results we estimated the mean free paths four our deposited layers. These values are found in table 6.

Table 6: Overview of the estimated mean free paths based on the residual resistivity from the deposited gold layers the Goddard group.

Layer Thickness (μm)	SRON			Goddard ^[12]	
	ρ at 4 K ($\mu\Omega\cdot\text{cm}$)		Mean free path (nm)	ρ at 4 K ($\mu\Omega\cdot\text{cm}$)	Mean free path (nm)
	<i>brightener</i>	<i>No brightener</i>			
0.94	-	-	-	0.12	1000
1.1	0.46	-	180	-	-
1.4	-	0.35	240	-	-
2.0	-	0.32	260	0.04	2000
2.1	0.43	-	260	-	-
4.3	0.32	-	260	0.05	1680

5.3 Surface scattering

When the mean free path becomes larger than half the thickness of the deposited gold layer the surface scattering of the conducting electrons will be the limiting factor on the residual resistivity.^[8] Based on this and the estimated mean free paths the influence of the layer thickness on the observed residual resistivity can be analyzed. The estimated mean free paths and the factor $t/2$ are given in table 7.

Table 7: Overview of the estimated mean free paths and factor $t/2$

		Layer thickness (μm)	l (nm)	$t/2$ (nm)
SRON	With brightener	1.1	180	500
		2.1	260	1000
		4.3	260	2000
	Without Brightener	1.4	240	700
		2	260	1000

For the deposited gold layers the factor $t/2$ is considerably larger than the estimated mean free path. The layer thickness is hereby not an limiting factor .

5.4 Estimation of the grain size

If we neglect the influence of the surface scattering the observed residual resistivity will be the observed resistivity. The ratio between the intrinsic resistivity ρ_0 and the total resistivity including grain boundary scattering ρ_g is related to the mean free path and the grain size by the model developed by Mayadas and Shatzkes^[15] and is described by Bernat.^[2]

$$\frac{\rho_0}{\rho_g} = 3 \left(\frac{1}{3} - \frac{1}{2} \alpha + \alpha^2 - \alpha^3 \cdot \ln \left(1 + \frac{1}{\alpha} \right) \right) \quad [18]$$

Where alpha is:

$$\alpha = \frac{l_0 R}{d (1-R)} \quad [19]$$

Where:

l_0	= Mean free path	[nm]
d	= Average grain size	[nm]
R	= Electron reflection coefficient at the grain boundary	

Mayadas and Shatzkes find that R for Cu and Al are around 0.2. Assuming the same R for gold the required grain size can be estimated. This is done by assuming the ratio ρ_0/ρ_g is 1 when the grain boundary scattering become the dominant factor in the residual resistivity. From this model we were able to estimate the grain sizes of the deposited gold layers and these are shown in table 8.

Table 8: estimated grain sizes based on the model from Mayadas and Shatzkes.

RRR	Mean free path (nm)	Grain size (nm)	remarks
6	180	70	With brightener
11	260	100	without brightener
50	2000	800	Minimal grain size required for these RRR values
100	4000	160	

The estimated values of the grain size for the sample deposited with brightener is below 100 nanometers. The observed surface of these samples showed small pits and bumps about the same size as these estimated grains. The grain size of the deposited samples without brightener is estimated to be around 100 nm. The observed surface of these samples shows large crystallite structures. These structures were observed to be far longer than their width and are estimated to be in the 100 to 200 nm range based on the SEM micrographs. The estimated grain sizes are thus roughly the same as the observed grain size.

From this we can attempt to predict the required grain sizes for RRR values of 50 and 100. These indications of minimal required grain sizes are needed to obtain the preferred residual resistivity.

5.5 further optimization

Based on the discussion we assume that the grain size is the key factor to lowering the resistivity at low temperature. Based on the initial depositions without brightener we believe there is room for improvement and further optimization of the plating conditions for the electrolyte without brightener is needed. Using the estimation of the RRR based on the grain size observed with SEM provides a valuable tool in the further optimization of the electroplating parameters.

6 Conclusion

In this thesis a description is given about the startup of the electroplating gold layers at SRON. A procedure is presented to characterize the plating bath and to establish stable and reproducible conditions for electrodeposition of gold layers with thickness of 500 nm till 4 micron.

Stable plating conditions were established by investigating some bath characterizations. Sufficient bath agitation (mechanically stirring above 500 rpm) is crucial to achieve uniform plating conditions and plating using a current biased power source resulted in better uniformity and reproducibility.

By varying the operational plating parameters during the deposition of gold we observed a lowest resistivity of around $3 \mu\Omega\text{-cm}$ for a current density of 1 mA/cm^2 at a bath temperature of 50 C Celsius.

The addition of brightener to the electrolyte leads to small grain sizes and a shiny polished surface of the gold layer. With no brightener the gold layers looked more coarse grained and resistivity at room temperature went slightly up to 3.2 to $4.2 \mu\Omega\text{-cm}$.

At cryogenic temperatures of 4 Kelvin we found RRR values varying from 6 to 11. The highest value was found for a gold layer plated without brightener in the electrolyte.

We compared our RRR values with other groups and found out that these are substantially lower than other groups has demonstrated (RRR variation from 24 – 50).

We have interpreted our resistivity data at low temperature in terms of grain sizes and concluded that there is room for improvement for the plating conditions, especially for the electrolyte without the brightener.

Literature

- [1] <http://www.the-athena-x-ray-observatory.eu/>
- [2] T.P. Bernat, N.B. Alexander and J.L. Kaae ; *Thermal and Electrical Conductivities of Electroplated Gold.*
- [3] A.-D. Brown, S.R. Bandler, R. Brekosky ; *Absorber Materials for Transition Edge Sensor X-ray Microcalorimeters.*
- [4] G.E. Childs, L.J. Ericks and R.L. Powell; *Thermal Conductivity of Solids at Room Temperature and Below. NBS Monograph 31, September 1973, p. 108*
- [5] R. E. Hummel, *Understanding Material Science*
- [6] Materials Science, fall 2008, part III Electromagnetic properties
- [7] Yan Wen, CHEN Jian and FAN Xin-hui, *Effects of grain boundaries on electrical properties of copper wires, Trans. Nonferrous Met. Soc. China Vol. 13 nr. 5 (October 2003)*
- [8] F. Lacey, *Developing a Theoretical relationship between electrical resistivity, temperature and film thickness for conductors. Nanoscale Reseach Letters 2011 6:636*
- [9] M Schwartz, *Deposition from Aqueous Solutions: an overview*
- [10] K. W. Yee, *Master Thesis: Gold-Electroplating Technology for X-Ray-Mask Fabrication, MIT June 1996*
- [11] R. E. Reed-Hill, *Physical Metallurgy Principles second Edition, IXO GSFC workshop, Jan 2009*
- [12] J.A. Chervenak, *Fabrication overview of Transition Edge Sensor x-ray calorimeter arrays,*
- [13] J.W. Dini, *Deposit Structure, Plating & Surface Finishing, 17, 11 Oct 1988*
- [14] Techni-gold 25 E S Data sheet
- [15] A.F. Mayadas M. Shatzkes, *Electrical-Resistivity Model for Polycrystalline Films: The Case of Arbitrary Reflection at External Surfaces, Phys. Rev. B1, 1382 (1970)*
- [16] M. Paunovic M Schlesinger, *Fundamentals of Electrochemical Deposition, Second Edittion*

Appendix

A. Originele opdracht omschrijving

SRON ontwikkelt en fabriceert beeldvormende cryogene sensoren voor toepassing in de röntgen en infrarood astronomie. Het werkingsprincipe van de sensoren is als volgt. Ieder pixel is een thermisch geïsoleerd eiland wat zo is gedimensioneerd dat het meetbaar opwarmt als de beoogde fotonen worden geabsorbeerd. Als thermometer wordt een supergeleider in de thermische overgang gebruikt, waar de weerstand sterk afhankelijk is van de temperatuur. Er wordt gebruik gemaakt van lithografische technieken in de clean room van SRON om de detectoren te fabriceren.

Om de detectoren optimaal te laten functioneren, is een snelle interne thermalisatie binnen het pixel een vereiste. Deze snelle thermalisatie willen we realiseren door gebruik te maken van een, nog te ontwikkelen, dunne goudlaag. De depositie techniek die hiervoor gebruikt zal worden is elektroplating.

De afstudeeropdracht omvat het optimaliseren van het elektroplating proces met als doel een goudlaag te ontwikkelen met de gewenste thermische eigenschappen op cryogene temperaturen.

Voor de afstudeeropdracht zal de afstudeerder grotendeels in de clean room werken aan een bestaande opstelling voor het elektroplaten van dunne goudlagen.

Wat de proces optimalisatie betreft zal het gaan om het onderzoeken van enkele bepalende elektroplatingsparameters als stroomdichtheid, pulsform en frequentie.

Wat betreft de analyse van de lagen zal het gaan om inspectie door gebruikmaking van in-huis technieken als optische microscopie en SEM microscopie. Indien nodig kan ook gebruik worden gemaakt van röntgen diffractie technieken. Aangezien de Ohmse weerstand van de goudlagen bepalend is voor de thermische eigenschappen van de laag zullen er weerstandsmetingen uitgevoerd worden zowel op kamertemperatuur als op 4 Kelvin,

Begeleiders:

Ing. Marcel Ridder

Dr.ir. Jan van der Kuur

Afstudeerperiode: 17 november 2014 – 20 maart 2015

B. Mathematical derivation of Electrical resistivity.

When an electric field is imposed the current will flow in response to it. Therefore is it more convenient to write equation [5] in the inverted form:

$$J = \sigma \cdot E \quad [7]$$

The force exerted by the electric field on the electron is equal to:

$$F = e \cdot E \quad [8]$$

where:

F	= Force	[N]
e	= Charge of an electron	$[-1.6 \cdot 10^{19} \text{ C}]$

This force accelerates the electron through the conducting material. Without the presence of an electric field the electron will still possess a velocity, which depends on the Fermi energy, called the Fermi velocity. however the net velocity of the electrons in the conducting material will be equal to zero since the electrons will move in random directions. The resulting average velocity of the electrons under the influence of an external electric field is called the drift velocity and is calculated as followed:

$$v = -\frac{F \cdot t}{m} = -\frac{e \cdot E \cdot t}{m} \quad [9]$$

where:

v	= Velocity of the electron	[m/s]
t	= Time	[s]
m	= Mass electron	$[9,11 \cdot 10^{-31} \text{ kg}]$

As discussed earlier the electrons moving through a conducting material will interact with imperfections and thermal vibrations in the crystal lattice. These interactions slow down the electron and equation [8] has to be written as:

$$v = -\frac{e \cdot \tau}{m} \cdot E = -\mu \cdot E \quad [10]$$

where:

2τ	= Average time of flight between collisions	[s]
μ	= Electron mobility	$[\text{m}^2/\text{Vs}]$

The net current density across a plane is the net number of electrons that cross per unit area per unit time and is as followed:

$$J = -n \cdot e \cdot v = \frac{n \cdot e^2 \cdot E \cdot \tau}{m} = n \cdot e \cdot \mu \cdot E \quad [11]$$

where:

n	= Density of mobile electrons
-----	-------------------------------

Combining equation [10] with Ohms law from equation [6] the following relation for the conductivity can be found:

$$\sigma = n \cdot e \cdot \mu \quad [12]$$

Equation [2] shows the two factors determining the conductivity of an material. The density of mobile electrons n is a characteristic of the material and determines if an material is inherently a good conductor. The second factor is the electron mobility which is in turn determined by the average time of flight between collisions of the free electrons.

C. Data sheet NB Semiplate AU 100

Technical datasheet



NB Semiplate Au 100

Fahrenheitstraße 1
28359 Bremen
Germany

NB SEMIPLATE AU 100

Au electroplating process

INTRODUCTION

NB SEMIPLATE AU 100 is an alkaline, non-cyanide electroplating formulation which produces a bright, ductile deposit. In comparison with other gold plating processes, the NB SEMIPLATE AU 100 electrolyte demonstrates exceptional throwing power that results in good coverage of recesses, holes and hollows of parts of complex geometry. Deposits from the NB SEMIPLATE AU 100 process also exhibit the unique ability to build brightness with increasing thickness. Specific gravity measurements of the deposit consistently show values of 19.1 which indicate freedom of codeposited polymers generally found in deposits from other systems of similar purity. NB SEMIPLATE AU 100 deposits have main applications in MEMS processing.

PHYSICAL PROPERTIES OF THE DEPOSIT

Purity	99.9%
Hardness	130 to 190 mHV _{0,020}
Contact Resistance	0.3 Milliohms*
Deposit weight for 2.5 microns (100 micro inches)	31.6 mg/in ² (4.9 mg/cm ²)

*Contact resistance measured by cross-wire method with 200 gram load.

MATERIALS REQUIRED

Product Name	Comment
NB Semiplate Au 100	
AU 100 B	<ul style="list-style-type: none">• Make up solution
AU 100 R	<ul style="list-style-type: none">• Contains all the materials needed to replenish the working solution
Au 100 BRIGHTENER	<ul style="list-style-type: none">• Brightening Agent• Concentrations of this additive can be varied in working solutions based on specific operating preferences
Au 100 CONDITIONER	<ul style="list-style-type: none">• Maintains the specific gravity of the solution and complexes the gold
Au 100 X COMPLEX	<ul style="list-style-type: none">• Gold complex
Sodium hydroxide (NaOH, reagent grade, 20% by volume)	<ul style="list-style-type: none">• Is required to raise the pH
Sulfuric acid (H ₂ SO ₄ , reagent grade, 5% by volume solution)	<ul style="list-style-type: none">• Is required to lower the pH

EQUIPMENT REQUIRED

Tanks (liners)	Polypropylene, CPVC, unfilled PVC, and plexiglass are recommended. Viton is a recommended gasket material. If any questions arise as to material compatibility, consult NB Technologies.
Leaching	Leach all tanks and peripheral equipment thoroughly prior to installation of this process.
Heating	Titanium, stainless steel (type 316)
Filtration	Continuous filtration is required. Fiberglass or cellulose can be used to obtain a clear filtrate after carbon treatment. Use properly leached Dynel, or polypropylene filter cartridges.
Rectifiers	Sufficient to develop more than the greatest direct current required with less than 5% ripple at the amperage used.
Anodes	platinated titanium
Ventilation	exhaust according to local regulations

BATH PARAMETERS

The following table shows the bath parameters, which should be maintained and checked with regular sample analysis.

	NBT analysis	Units	Max. upper limit	Upper action limit	Optimum	Lower action limit	Lowest limit
Au	X	g/l	14	13,0	12,0	11	10,0
BRIGHTENER NO 6	X	ml/l	80	75	65	55	50
Density	-	g/cm ³	1,24	1,22	1,2	1,19	1,18
pH	(X)	pH	9,5	9,5	9,35	9,2	9,1
Stress level	-	MPa	50	20	0	-40	-80

GENERAL PLATING CONDITIONS

Parameter		Optimum	Range
Cathode current density	[mA/cm ²]	1,5	1 – 6
Flow depending on tool	[l/h]	-	1200 –
Anode to cathode spacing (depends on tool and wafer size)	[cm]		5 - 15
Temperature	[°C]	30	RT to 50

MAKE-UP PROCEDURE

To make up 5 litres of working solution the following are required:

AU 100 "B"	1 Unit (3 litre)
Au 100 X COMPLEX	600 mL (60 g Au)
BRIGHTENER NO 6	325 mL

AU 100 B (1 Unit = 3 litres)	Containing the additives necessary (except Au 100 BRIGHTENER) for 5 litres solution but not containing gold
Au 100 BRIGHTENER	Supplied separately in the current proportion for each "B-Unit" (65mL per "B-Unit") The necessary amount of gold for the installation is delivered as Au 100 X
Au 100 X COMPLEX	COMPLEX. The Au 100 X COMPLEX is supplied in 1 litre units containing 100g Gold.

1. Thoroughly clean the plating tank and fill to ¼ of the required final volume with deionised water.
2. Heat to 50°C and add the "B" unit liquid concent rate. Au 100 BRIGHTENER, which is delivered separately, is also added at this stage.
3. Add the necessary Au 100 X COMPLEX gold complex to give the final gold metal concentration required.
4. Adjust to final volume with deionised water.
5. Check and adjust density if necessary
6. Check and adjust the pH and temperature if necessary.

The solution is then ready for use.

SPECIFIC PROCEDURES

- Oxygen plasma before plating
- chemical pre-treatment not recommended/needed
- Cleaning of all items with DI before insertion in electrolyte
- Wetting of wafer surface with DI water before insertion into bath (check for wetting)
- 1 minute dwelling in bath before current application

SPECIFIC REQUIREMENTS

- Fixtures and anode should be operated in symmetric conditions to the wafer centre (distance of wafer edge to fixture edge, distance of fixture to tank wall, electrical contacting)
- Anode material platinated titanium
- Fixture and others features of PP, PFTE, POM or compatible-proven materials (degreased, leached)

OPERATION

Consistently optimum deposits from the NB SEMIPLATE AU 100 process are easily achieved through conscientious process control. Continuous filtration, vigorous mechanical (not air) agitation and good temperature control are important as well as careful rinsing techniques and the use of a gold strike. Brightness of the deposit from the NB SEMIPLATE AU 100 process must be maintained. A dull deposit is indicative of process imbalance and will eventually result in decomposition of the solution. To maintain deposit brightness, the gold concentration must be maintained within the specified range. If brightness has been lost, add Au 100 BRIGHTENER. If this addition is ineffective, make an addition of Au 100 CONDITIONER NO 6.

If satisfactory results are not obtained, other problems exist with the solution such as metallic and/or organic contamination or a specific gravity in excess of 1,261g/l.

NOTE: The concentration of conducting salts cannot be readily determined by measuring the specific gravity of the solution because they transform with bath use and time. Periodically send a sample of the solution to NB Technologies for analysis of conducting salts concentration.

MAINTENANCE

Routinely analyze the plating solution for gold concentration to determine the need for replenishment or to verify the accuracy of a replenishment schedule based upon Ampere-minutes of use. A gravimetric procedure for determining the concentration of gold in the solution is available through NB Technologies.

Gold concentration**Actions on Au concentration according to analysis:**

- o At lower action limit, at lowest limit at the latest, add correspondent amount of Au to the bath
- o At upper action limit reduce adding of Au on Amin-basis
- o At maximum upper limit stop adding of Au on Amin-basis

Replenishment of Au according to analysis:

- o 10ml Au 100 X per 1g of Au to be added
- o ≥ 1 ml AU 100 R per 1g Au added before

Replenishment of Au on Amin basis:

Beside analysis result, Au can be replenished on the basis of Amin plated.

- 45 litres bath: Every 180Amin plated replenish
- o 225ml of Au100 X (equalling 22.5 g Au)
 - o ≥ 22.5 ml AU 100 R

Au 100 BRIGHTENER**Actions on Au 100 Brightener according to analysis:**

- o At lowest limit add correspondent amount of Au 100 Brightener and increase adding of Au 100 Brightener on Amin-basis
- o At lower limit increase adding of Au 100 Brightener on Amin-basis
- o At upper action limit reduce adding of Au 100 Brightener on Amin-basis
- o At maximum upper limit stop adding of Au 100 Brightener on Amin-basis

Replenishment of Au 100 Brightener on the basis of time and/or Amin

The replenishment need of Au 100 Brightener is influenced on the conditions of oxygen entrapping into the electrolyte. This is a value of experience and conditions of individual tooling, condition of flow and Amin plated. When flow is minor or turned off for a longer period, there is no need to replenish. Replenishment of Au 100 Brightener on mere time basis is not recommended in the initial phase. In order to find out the individual amount of replenishment influenced by Amin and time, sample analysis correlation over several weeks of operation is needed. After gaining the replenishment correlation per week operation, the replenishment can be performed on Amin. The time plan for analysis control can be less tight.

Replenishment of Au 100 Brightener on the basis of optical inspection.

When the surface roughness is not satisfactory, the smoothness can be regained by adding Au 100 Brightener. This method might be needed especially during the correlation finding phase.

Provided prerequisites:

1. The surface condition is not caused by other effects (impurities, particles, etc).
 2. The Au 100 Brightener concentration is securely far from the maximum upper limit.
- Add 20ml/l Au 100 Brightener, until surface gets rid of unsatisfactory roughness.

Control of density and replenishment of conduction salt

Density may be reduced by drag out and fill up with DI-water. Density is to be measured in g/cm³ using a density meter with adequate measurement sensitivity. At 1,261g/cm³ the solution may be needed to be dumped.

Actions on density measurement results:

Make sure Au concentration is within the specified range.

- At lower action limit, at lowest limit at the latest, add 5g/l Au 100 Conditioner incrementally to avoid overshooting 1,261g/cm³. Dissolve at elevated temperatures (45-55°C).
- At upper action limit intensify measurement cycles
- At maximum upper limit dilute solution to optimum level, analyse diluted solution and replenish according analysis result

pH control and adjustment

During operation the pH tends to drop. pH may never drop lower than 8, or the Au complex may fall out. Proper operation is provided in the specified range only. At pH over 10, photo resist stability may be affected depending on the type of material.

Actions on pH measurement results:

Make sure to agitate properly during adjustments:

- o At lower action limit, at lowest limit at the latest, raise pH by adding 5 to 20% NaOH (100ml NaOH (5%) is common to raise pH from 9,2 to 9,35 in 45 liter bath)
- o At maximum upper limit, lower the pH by adding 5% sulphuric acid. This normally is not needed or occurs at new mixture only.

Do not use higher concentrations to avoid localised pH drop down lower than pH 8 during addition.

Stress measurement

Stress can be evaluated by sheet film deposition and measurement of the change of wafer bow.

Usual stress level for 7µm film plated at 1,5mA/cm²:

-40MPa compressive Stress level tends to drop in tensile direction over operation time

Actions on stress measurement results:

From mechanical perspective the bath can be operated within in the maximum ranges. Still, reaching the ranges is a sign of poor condition of the bath, which gives motivation to set up a new bath. There are no replenishers to adjust stress specifically.

- o At lower and upper action limit, check for improper conditions of bath and tool
- o At maximum and minimum action limit, and after excluding abnormal tool conditions, consider to perform carbon filtering or to dump the solution right away and reclaim the Au.

Carbon filtering

In order to remove organic contaminations as per analysis or by suspect, organic cleaning and carbon filtering may be applied. After the procedure, analysis and replenishment of the additioners is required. Regular carbon filtering is not recommended. Contact NB Technologies for technical assistance.

Impurities

Introduction of metallic impurities into the solution should be prevented by proper rinsing of the parts to be plated. The NB SEMIPLATE AU 100 process is relative tolerant to low levels of heavy metal contaminants, as it will codeposit these metals without serious effect upon either the appearance or physical properties of the deposit. Organic impurities may be dragged into the plating solution from a variety of sources and will usually result in a significant decrease in plating efficiency which will eventually lead to bath decomposition.

D. Technical data Autolab PGSTAT204

Table 9: Technical data of Autolab PGSTAT 204

Autolab PGSTAT204	
Electrode connections	2, 3 and 4
Potential range	+/- 10 V
Compliance voltage	+/- 20 V
Maximum current	+/- 400 mA
Current ranges	100 mA to 10 nA
Potential accuracy	+/- 0.2 %
Potential resolution	3 μ V
Current accuracy	+/- 0.2 %
Current resolution	0.0003 % (of current range)
Input impedance	> 100 GOhm
Potentiostat bandwidth	1 MHz
Computer interface	USB
Control software	NOVA

E. Measured data of deposited test structures

Table 10: Data of the samples deposited using an voltage biased power source

Voltage (V)	Plating time (sec)	Bath temperature (C)	thickness measured (nm)	thickness plated layer (nm)	plating rate (nm/sec)	measured width (Pix)	structure dimensions (μm)	amount of squares	R measured @ 293K in Ohm	R corrected for seed layer	R square @ 293K in Ohm/sqr	Rho @ 293 K (micoOhm-cm)
0.55	200	20	300	219	1.10	31.6	33.2	121	17.00	24.225	0.201	4.40
0.55	400	20	525	444	1.11	37.1	39.0	103	8.30	9.715	0.095	4.20
0.55	800	20	950	869	1.09	32.5	34.1	117	5.06	5.722	0.049	4.24
0.55	800	20	980	899	1.12	34.5	36.2	110	3.79	4.060	0.037	3.31
0.575	120	20	204	123	1.03	37.2	39.1	102	23.55	31.384	0.306	3.77
0.575	400	20	780	699	1.75	34.3	36.0	111	5.77	6.416	0.058	4.04
0.575	800	20	1420	1339	1.67	35	36.8	109	3.35	3.559	0.033	4.38
0.575	300	20	550	469	1.56	37.4	39.3	102	8.40	9.855	0.097	4.54
0.575	800	20	1355	1274	1.59	32	33.6	119	4.65	5.063	0.043	5.42

Table 11: Data of the samples deposited using an current biased power source

current density (mA/cm ²)	Plating time (sec)	Bath temperature (C)	thickness measured (nm)	thickness plated layer (nm)	plating rate (nm/sec)	measured width (Pix)	structure dimensions (μm)	amount of squares	R measured @ 293K (Ω)	R corrected (Ω)	R square @ 293K (Ω/sqr)	ρ @ 293K (μΩ-cm)
0.25	2000	20	610	529	0.26	35.0	36.8	109	6.70	7.59	0.070	3.69
0.25	2000	30	650	569	0.28	35.0	36.8	109	6.16	6.90	0.063	3.61
0.25	2000	40	638	557	0.28	35.5	37.3	107	5.78	6.43	0.060	3.34
0.25	2000	50	652	571	0.29	33.3	35.0	114	6.00	6.70	0.059	3.34
0.25	2000	60	690	623	0.31	35.4	37.2	108	6.31	6.89	0.064	3.99
0.5	900	20	570	489	0.54	35.0	36.8	109	7.72	8.93	0.082	4.01
0.5	1000	20	627	546	0.55	34.0	35.7	112	7.01	7.99	0.071	3.89
0.5	1000	30	635	554	0.55	34.0	35.7	112	6.31	7.09	0.063	3.51
0.5	1000	40	615	534	0.53	34.0	35.7	112	6.17	6.92	0.062	3.30
0.5	1000	50	643	562	0.56	34.5	36.2	110	5.59	6.19	0.056	3.15
0.5	1000	60	650	586	0.59	36.0	37.8	106	5.37	5.78	0.055	3.20
1	500	20	620	539	1.08	33.6	35.3	113	7.40	8.50	0.075	4.04
1	500	30	635	554	1.11	35.0	36.8	109	6.31	7.09	0.065	3.61
1	500	40	638	557	1.11	35.0	36.8	109	5.73	6.37	0.059	3.26
1	500	50	620	539	1.08	35.0	36.8	109	5.58	6.18	0.057	3.06
1	1000	50	1142	1061	1.06	31.0	32.6	123	3.09	3.27	0.027	2.82
1	2000	50	2200	2119	1.06	32.0	33.6	119	1.54	1.58	0.013	2.82
1	4300	50	4640	4559	1.06	29.2	30.7	130	0.78	0.79	0.006	2.75
1	500	60	630	549	1.10	34.4	36.1	111	5.73	6.37	0.058	3.16
1	1000	60	1160	1096	1.10	35.6	37.4	107	2.67	2.77	0.026	2.83
1.5	375	25	655	588	1.57	36.0	37.8	106	6.53	7.15	0.068	3.97
1.5	375	30	665	598	1.59	36.4	38.2	105	5.97	6.49	0.062	3.71
1.5	375	40	690	623	1.66	36.6	38.4	104	5.15	5.53	0.053	3.31
1.5	375	50	666	585	1.56	35.0	36.8	109	5.27	5.81	0.053	3.12
1.5	375	60	685	618	1.65	35.0	36.8	109	4.98	5.33	0.049	3.03
2	250	25	600	536	2.14	36.4	38.2	105	7.52	8.36	0.080	4.28
2	250	30	610	543	2.17	35.4	37.2	108	6.81	7.49	0.070	3.78
2	250	40	625	561	2.24	36.4	38.2	105	5.95	6.46	0.062	3.46
2	250	50	610	529	2.12	34.0	35.7	112	6.04	6.76	0.060	3.19
2	250	60	620	553	2.21	35.4	37.2	108	5.64	6.10	0.057	3.14